การสังเคราะห์และการอัดอนุภาคนาโนของเงินบนผ้าฝ้ายและสมบัติการต้านแบคทีเรีย

นางสาวปาริชาต สุดสุริยะ

SYNTHESIS AND PADDING OF SILVER NANOPARTICLES ON COTTON

FABRIC AND THEIR ANTIBACTERIAL PROPERTY

Miss Parichat Sudsuriya

A Thesis Submitted in Partial Fulfillment of the Requirements

for the Degree of Master of Science Program in Petrochemistry and Polymer Science

Faculty of Science

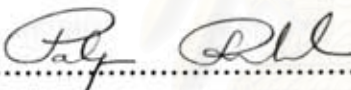Chulalongkorn University

Academic Year 2008

Thesis Title   SYNTHESIS AND PADDING OF SILVER NANOPARTICLES ON COTTON AND THEIR ANTIBACTERIAL PROPERTY

By   Miss Parichat Sudsuriya

Field of Study Chemistry

Thesis Advisor Associate Professor Sanong Ekgasit, Ph.D.

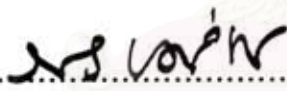Thesis Co-advisor Associate Professor Chuchaat Thammacharoen

---

Accepted by the Faculty of Science, Chulalongkorn University in Partial Fulfillment of the Requirements for Master's Degree

..............Vimolvan Pimpan...............Deputy Dean of Administrative Affairs,

Acting Dean, The Faculty of Science

(Associate Professor Vimolvan Pimpan, Ph.D.)

THESIS COMMITTEE

....Chairman

(Professor Pattarapan Prasassarakich, Ph.D.)

....Thesis Advisor

(Associate Professor Sanong Ekgasit, Ph.D.)

....Thesis Co-advisor

(Associate Professor Chuchaat Thammacharoen)
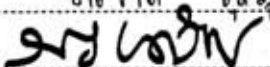
....Member

(Associate Professor Supason Wanichwecharungruang, Ph.D.)

....Member

(Assistant Professor Varawut Tangpasuthadol, Ph.D.)

ปาริชาต สุคสุริยะ : การสังเคราะห์และการอัคอนุภาคนาโนของเงินลงบนผ้าฝ้ายและสมบัติการ
ด้านแบคทีเรีย (SYNTHESIS AND PADDING OF SILVER NANOPARTICLES ON COTTON
AND THEIR ANTIBACTERIAL PROPERTY) อ.ที่ปรึกษา: รศ. คร. สนอง เอกสิทธิ์, อ.ที่ปรึกษา
ร่วม: รศ. ชูชาติ ธรรมเจริญ, 79 หน้า.

อนุภาคนาโนของเงินที่มีความเข้มข้นสูง (10,000   ส่วนในล้านส่วน) และมีเสถียรภาพสูง
สังเคราะห์โดยวิธีรีดักชันเกลือซิลเวอร์ด้วยโซเดียมโบโรไฮไครค์ในสภาวะที่มีสารคงสภาพ โดยสารคง
สภาพที่ใช้คือ พอลิไวนิลไพรโรลิโดน , เจลาติน และ แป้ง การตรวจสอบขนาดและการกระจายตัวของ
ขนาดอนุภาคนาโนของเงินด้วยเทคนิคยูวีวิสิเบิลสเปคโตรสโกปีและกล้องจุลทรรศน์อิเล็กตรอนแบบส่อง
ผ่าน (TEM) พบว่าอนุภาคนาโนของเงินที่อยู่ในสารละลายแป้งจะมีขนาดเล็กและการกระจายตัวแคบกว่า
อนุภาคนาโนของเงินในสารละลายเจลาตินและสารละลายพอลิไวนิลไพรโรลิโดน อนุภาคนาโนของเงิน
ในสารละลายแป้งจะถูกตรึงลงบนผ้าฝ้ายและผ้าโพลีเอสเทอร์ด้วยกระบวนการอัด วิธีนี้เป็นวิธีที่ง่ายและ
สะควกในการนำไปประยุกต์ใช้ในโรงงานอุตสาหกรรมสิ่งทอ เนื่องจากไม่ต้องเปลี่ยนแปลงกระบวนการ
ผลิตและเครื่องจักรของโรงงาน โดยลูกกลิ้งในกระบวนการอัดมีการควบคุมแรงกด เพื่อควบคุมปริมาณ
ของคอลลอยด์น้ำของอนุภาคนาโนของเงินบนผ้า ผลจากการศึกษาด้วยเครื่องอิเล็กตรอนแบบส่องกราด
ยืนยันการเกาะติดของอนุภาคนาโนของเงินบนผ้า สมบัติการด้านแบคทีเรียของอนุภาคนาโนของเงินบน
ผ้าถูกทดสอบโดย AATCC test method 147-1998 ของ the American Association of Textiles Chemist
and Colorists พบว่าอนุภาคนาโนของเงินมีฤทธิ์ด้านการเจริญเติบโตของเชื้อแบคทีเรียได้ดี

สาขาวิชา   ปิโตรเคมีและวิทยาศาสตร์พอลิเมอร์   ลายมือชื่อนิสิต   ปาริชาต   สุคสุริยะ
ปีการศึกษา   2551   ลายมือชื่ออาจารย์ที่ปรึกษา

4872368723 : MAJOR PETROCHEMISTRY AND POLYMER SCIENCE
KEY WORD: SYNTHESIS/ PADDING/ STABILIZER/ SILVER NANOPARTICLES

PARICHAT SUDSURIYA: SYNTHESIS AND PADDING OF SILVER NANOPARTICLES ON COTTON AND THEIR ANTIBACTERIAL PROPERTY. THESIS ADVISOR: ASSOC. PROF. SANONG EKGASIT, PH.D., THESIS CO-ADVISOR: ASSOC. PROF. CHUCHAAT THAMMACHAROEN, 79 pp.

Highly concentrated (10,000 ppm) and highly stabilized colloidal silver nanoparticles were synthesized by reduction of silver salt with borohydride in the presence of a stabilizer. The stabilizer used is a biocompatible material including gelatin, polyvinylpyrrolidone (PVP), and starch. The efficiency of these stabilizers was investigated. The size, size distribution and morphology of nanoparticles were characterized by UV/visible spectroscopy and transmission electron microscopy (TEM). The silver nanoparticles with starch as a stabilizer have the smallest particle size and narrowest particle size distribution. Immobilization of silver nanoparticles on cotton and polyester fabrics was carried out by padding method by silver nanoparticles with starch. This method is simple and easily performed without any change of the machine in factories. Padding pressure was adjusted in order to control the amount and uniformity of silver nanoparticles on the fabrics. Scanning electron microscope (SEM) images showed that silver nanoparticles were immobilized on the surface of the fabrics. The antibacterial properties of silver nanoparticles on the fabrics were investigated against *S. aureus* by AATCC test method 147-1998 (the American Association of Textiles Chemist and Colorists). The silver nanoparticles-immobilized fabrics showed excellent the antibacterial property.

Field of study Petrochemistry and Polymer Science   Student's signature ปริชาต รุตรุริยา

Academic year   2008   Advisor's signature หนง ผมา

ACKNOWLEDGEMENTS

CONTENTS

LIST OF FIGURES

Figure   Page

LIST OF TABLES

LIST OF ABBREVIATIONS

ppm	: part per million
PVP	: polyvinylpyrrolidone
TEM	: Transmission electron microscopy
SEM	: Scanning electron microscopy
S. aureus	: *Staphylococcus aureus*
SPR	: surface plasmon resonance
LSPR	: Localized surface plasmon resonance
nm	: nanometer
MBH_4	: tetrahydroborates of alkali metals
CMC	: carboxylmethyl cellulose
wt%	: weight percent
SERS	: surface-enhanced Raman scattering
AgNPs	: silver nanoparticles
$AgNO_3$	: silver nitrate
$NaBH_4$	: sodium borohydride
kV	: kilo volt
FWHH	: Full width at half height
SERRS	: surface-enhanced resonance Raman scattering
RhBITC	: rhodamine B isothiocyanate
PAA	: poly(acrylic acid)
PAH	: poly(allylamine hydrochloride)

LIST OF SYMBOL

E	: redox potential of particles
Ag	: silver
λ_{max}	: plasmon extinction mamximam
℃	: degree Celsius

CHAPTER I

INTRODUCTION

For a long time, material coating by antibiotics and antiseptics have been employed for the reduction of microorganisms. Several places such as hospital, house, or public places are used these materials. Due to increasing bacterial resistance to antibiotics and antiseptics, nanotechnology may be an effective device to prevent bacteria and pathogenic fungi. Nanotechnology is the science of making or working with things that are so small that they can only be seen using a powerful microscope and it is related to size of material or phenomena in nano-scale, its fabrication, properties and their applications. In the past, the production of nanomaterial was produced from top-down management by creating instrument and constructed large material to small material. At this time, top to bottom production is changed into bottom-up methodology which is producing in atomic/molecular level. Silver nanoparticle is a class of nanomaterial which exhibits the antibacterial properties. It is used to replace the antibiotics because nanoparticles attack a board range of targets in the organism.

1.1   Nanoparticles

A nanoparticle is a small particle or cluster with one or more dimension as small as one nanometer to that of as large as several hundred nanometers in diameter. Novel properties of nanoparticle such as catalytic activity, optical properties, antimicrobial activity, and magnetic properties are distinctly different from its bulk counterpart. At the nano-scale, these properties of nanoparticle highly depend on their size and shape. For example, gold nanoparticles have deep red to black color in solution, which is different from bulk gold [1].

In the 9th century Mesopotamia, artisans used nanoparticles for making a glittering effect on the surface of pottery. This effect is called "Lustre" which is caused by a metallic film. Silver and copper salts and oxides with vinegar, ochre, and clay were together mixed in the glassy matrix of glazed pottery. And then it was heated at 600°C with a reducing atmosphere in the kiln. The silver and copper ions migrated into the outer layers of the glaze since the glaze would soften when it was heating. These ions were reduced and became silver and copper nanoparticles, which giving unique color and optical effects. The lustre was occurred from these nanoparticles within the film.

Nowadays, nanoparticles are attracting a great of scientific interest because of their potential properties for achieving specific purposes. Nanoparticles posses a high surface to volume ratio which can use in a variety of application such as semiconductor technology, magnetic storage, electronics fabrication, reaction catalysis, environmental, and pharmaceutical applications. For example, the extremely small size of nanoparticles have melting point drastically lower than its bulk because of the surface energy of the nanoparticles enormously increasing. Advantages of the low melting point of the metallic nanoparticles, it is possible to fabricate micro-interconnects by ink-jet printing metallic nanoparticles suspensions on substrates at low sintering temperature with a short period of time.

A: B:
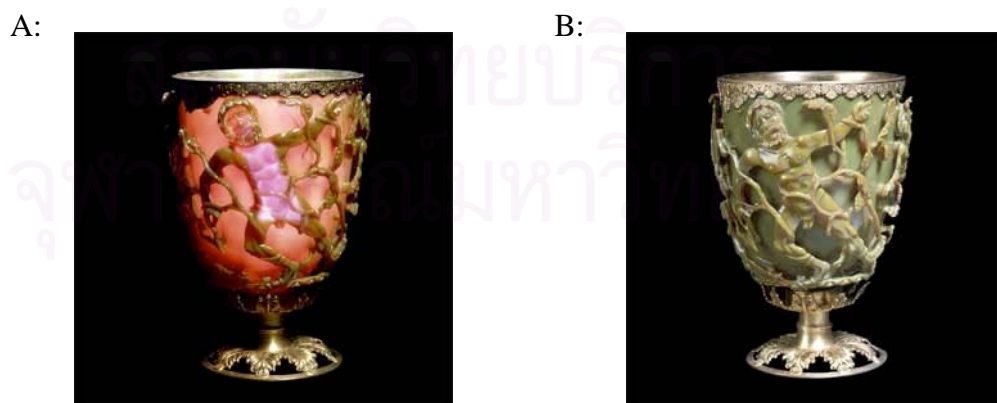
Figure 1.1   Lycurgus cup which contained metal nanoparticles, gold and silver, when light is transmitted through the glass it appears red (A) and when light is scattered near the surface it appears greenish (B).

1.2   Silver and silver nanoparticle

Silver is a white and shinny metallic element. Silver is positioned on 47th in the Periodic Table. Silver has a latin name as "argentum" and Ag as its chemical symbol. The properties of pure silver are ductile and malleable which sintering for silverware. Furthermore, Silver has the highest electrical and thermal conductivity over any metal as well as the lowest contact resistance. For centuries, silver has been widely used in human life such as jewelry, monetary currency, dental alloy, photography, or antibacterial agent. In the case of antibacterial agent, silver has been employed to treat disease and control spoilage. Since lungs, the gastrointestinal tract, and tissues can be absorbed silver by becoming silver sulfite. When an excessive amount of silver is absorbed, it will form a complex in elastic fibers. Consequently, the skin and eyes will be bluish, grey-blue, or a black color for over dose. This condition is called "argyria or argyrosis". Although it is not a toxic effect, argyria is undesirable and usually permanent [2]. Thus silver was declined away as an antimicrobial agent. When modern science is widely developed, metallic silver is performed with new technologies, leading to novel morphologies and properties. Therefore, metallic silver is managed into ultrafine particles which is called "silver nanoparticle". The properties of silver in nano-scale are different from its bulk. For example, silver metal is grayish while colloidal silver nanoparticle is a clear yellow.

Silver nanoparticles display remarkably physico-chemical properties and biological activities including catalysis, magnetic and optical polarizability, electrical conductivity, and antibacterial activity [3-5]. From these properties, silver nanoparticles are employed in several applications. Silver nanoparticles were integrated in medical device, laundry detergents, water purificants, and washing machine. In addition, the manufacture of textile such as clothing and underwear used silver nanoparticles incorporating in the fabrics as an antibacterial agent [6].

A: bulk silver   B: colloidal silver nanoparticle

Figure 1.2   The properties of metallic silver and silver nanoparticle are different
                which the silver bulk is grayish (A) and colloidal silver nanoparticle is
                a clear yellow (B).

From these several applications, the developments of silver nanoparticles synthetic methods have been studied in order to control the nanoparticle size. Controlling of nanoparticle morphology has proved more difficult to achieve. Many methods for the preparation of silver nanoparticles have been reported [7-10]. Some methods are suitable for only some application. In some application such as sensor, it may be desirable to have smaller-size nanoparticles and rod shape. The synthesis of silver nanoparticles with rod shape was used by the reduction method which sodium borohydride as a reducing agent and citrate as a stabilizer. Surfactant must use in this method for getting rod shape [11]. The other methods for example the electro-chemical [12], seed-mediated growth [13], and ultraviolet irradiation-photoreduction [14] methods were also reported. For other applications such as silver paste, larger-size nanoparticles may be desired. The silver nanoparticles were prepared by the chemical reduction method. The synthesis used tri-sodium citrate as a surfactant and hydrazine monohydrate as a reducing method [15]. Additionally, for some applications such as antibacterial agent it may be preferred the nanoparticles in a smaller-size, spherical shape and unagglomerated because the smaller nanoparticle having higher efficiency due to the particle has a very high surface area [16-18]. The spherical colloidal silver nanoparticles may be synthesized by the reduction method

which has sodium borohydride as a reducing agent in the presence of the stabilizer or surfactant owing to sodium borohydride is a strong reducing agent.

However, the most researchers described procedures to synthesize stable silver colloids only at low concentrations of metal, so they are not suitable for large-scale manufacturing. Very few number of researchers described highly concentrated and stable dispersions of silver nanoparticles. Stable concentrated dispersions of silver nanoparticles were synthesized by reduction of silver nitrate with ascorbic acid in the presence of 5 wt% Daxad 19 (sodium salt of a high molecular weight naphthalene sulfonate formaldehyde condensate) as a stabilizer. Daxad 19 prevented the aggregation of silver nanoparticles at high concentration of metal up to 0.3 mol/L in the final volume of 100 mL (27,000 ppm). The size distributions were narrow and average sizes of the synthesized silver nanoparticles after 1 min and after completion of the process (7min) were 15 and 26 nm, respectively. However, surfactant and some parameters were rather restrictive for these experimental [19]. The synthesis of high concentration of silver colloidal nanoparticles by chemical reduction of silver ions in the presence of laponite using sodium borohydride as the reducing agent were described. The concentration of silver nanoparticles was depended on concentrations of silver nitrate. The concentration of silver nanoparticle was 245 ppm. Silver nanoparticles with laponite as a stabilizer were suitable to apply in human use applications, since laponite is nontoxic and environmentally inert material [20]. A process for preparing silver nanoparticles can be synthesized by reducing silver acetate with surfactant. Sodium n-octane sulfate (SOS) was used as surfactant and reducing agent. The reducing reaction of silver salt by SOS can be carried out under reflux at a temperature of 120°C for 18 hours. The concentration of the synthesized silver nanoparticles was about 15,500 ppm. From the results revealed that reducing power of SOS was depend on the carbon chain length of the lipophilic group. This process was not limited by the size of the reactor and suitable to transfer to the manufacturing for synthesis in large mass scale production [21].

The immobilization of silver nanoparticles on material has been interested in many fields. In textile industry, silver nanoparticles have been employed the

antibacterial agent. So the simple process at low processing cost and the least limitations for some companied was required to obtain the desired quality products. This method is the padding process which is in finishing process. This process is a suitable process for application of textile industry because it is simple and does not change the process or the machine of factory.

In order to control size of silver nanoparticles, chemical reduction method by using sodium borohydride as a strong reducing agent in the presence of a stabilizer is developed. This method is simple and can be desired to have smaller-size and highly concentration of silver nanoparticles for bacterial agent in application of textile industries. The method for immobilization on the fabrics is "padding process". In padding process, padder or roller was used to control amount and uniformity of silver nanoparticles on the fabrics.

1.3   Objective of the research work

The purposes of this research are to develop the method to synthesize a stable and highly concentrated (10,000 ppm) colloidal silver nanoparticles by the chemical reduction method. Colloidal silver nanoparticles were prepared by reducing silver nitrate solution using sodium borohydride in the presence of a stabilizer. Stabilizer that we used is a biocompatible material which can be applied in cosmetics and food packaging without unreasonable risks to people and environment. Immobilization of silver nanoparticles on cotton and polyester were carried out by padding process. Immobilization of silver nanoparticles on the fabrics was studied and the antibacterial properties of silver nanoparticles on the fabrics were studied to confirm immobilization of silver nanoparticles.

1.4   Scopes of the research

This research is divided into three steps. Firstly, highly concentrated silver nanoparticles are synthesized by chemical reduction method using sodium borohydride as a reducing agent. Polyvinylpyrrolidone (PVP), gelatin, and starch are

investigated for suitable stabilizer. The particles size, shape, and size distribution of silver nanoparticles are characterized by UV-Visible spectroscopy, transmission electron microscopy (TEM). Secondly, the smallest silver nanoparticles colloid having a very narrow size distribution and highly stabilization is used in the padding process for immobilization them on cotton and polyester fabrics. Cotton and polyester fabrics are padded through silver solution bath which the dispersion, immobilization, and morphology of silver nanoparticles on the fabrics were observed by SEM. Lastly, the antibacterial efficacy of silver nanoparticles on cotton and polyester fabric is studied to confirm the immobilization of silver nanoparticles on fabrics. The fabrics are laundered at 20 times washing before antibacterial test. The antibacterial properties are evaluated against a Gram-positive bacteria, *Staphylococcus aureus* (*S. aureus*) by AATCC test method 147-1998 of the American Association of Textiles Chemist and Colorists.

CHAPTER II

THEORETICAL BACKGROUND

This chapter describes the fundamentals of surface plasmon resonance spectroscopy of metal nanoparticle. Surface plasmons are not only the modes supported by thin metal films, but also by small metal particles where they cause peculiar optical properties. To understand these optical properties and phenomena of metal nanoparticles, the Maxwell's equations are the starting equation for determining all classical electromagnetic effect. Furthermore, the synthesis and application of the silver nanoparticles were described.

2.1 Principles of the light interaction with metals nanoparticles

2.1.1 The classical theory: Maxwell's equation and electromagnetic wave propagation

Maxwell's equations can be clearly described the interaction of metals with electromagnetic field. Even metals nanoparticle with a few nanometer in size can be described. Maxwell's equations for light propagating are given by Equation 2.1 to Equation 2.4 [22].

$$\nabla \cdot D = \rho_{ext} \qquad 2.1$$

$$\nabla \cdot B = 0 \qquad 2.2$$

$$\nabla \times E = -\frac{\partial B}{\partial t} \qquad 2.3$$

$$\nabla \times H = J_{ext} + \frac{\partial D}{\partial t} \qquad 2.4$$

where D is dielectric displacement, B is the magnetic induction or magnetic flux density, E is the electric fields, H is the magnetic field, ρ_{ext} is external charge, and J_{ext} is the current densities. These fields are further linked with the dielectric constant, ε,

and permeability, μ. In general the dielectric constant and the magnetic permeability are dependent on the intensity of the field applied. The relations of the dielectric constant and the magnetic permeability between the intensity of the applied field are given by Equation 2.5. However, these equations are of limitation use by themselves to linear, isotropic and nonmagnetic media. In order to real problems, relations describing the response of the materials involved are given by Equation 2.6, the so-call constitutive relations.

$$H = \mu_0^{-1} B - M \qquad \text{and} \qquad D = \varepsilon_0 E + P \qquad\qquad 2.5$$

$$P = \varepsilon_0 \chi E, \qquad H = \mu_0^{-1} B - M, \qquad J = \sigma E \qquad\qquad 2.6$$

where M is the magnetization, ε_0 and μ_0 are the electric permittivity and magnetic permeability of vacuum, respectively. J is the internal current density and the coefficients σ, μ, and χ are conductivity, permeability and dielectric susceptibility, respectively. Introducing these equations into the Maxwell's Equations, leads to the wave equation in Equation 2.7. These set of equations are sufficient to solve the time and spatial evolution of electromagnetic fields in the presence of metals [22].

$$\nabla^2 E = \mu_0 \varepsilon_0 \varepsilon_r \frac{\partial^2 E}{\partial t^2} \qquad\qquad 2.7$$

2.1.2   Light interaction with small particles

When electromagnetic field is applied to a particle, its electron under these action start to oscillate, the energy from the incident electromagnetic wave transforms into, for example, thermal energy in an absorption process. Some electrons can also be accelerated and then they can radiate energy in a scattering process. The sum of absorption and scattering of an electromagnetic wave through a material is called the electromagnetic extinction.

The extinction, σ_{ext}, in Equation 2.8 can be modeled as the optical response of one immersed nanoparticle times the particles concentration.

$$\sigma_{ext} = N(C_{abs} + C_{sca}) \qquad\qquad 2.8$$

where N is the number of particles per unit volume and C_{abs} and C_{sca} are the absorption and scattering cross sections of a single particle. The optical properties of a nanoparticle can be described in term of dielectric function $\varepsilon(\omega)$ which is obtained by solving the Maxwell Equations in matter. Gustav Mie found the exact solution from Maxwell Equations for the optical response of a spherical nanoparticle in a homogeneous medium in 1908. A dielectric function of nanoparticle is used to find the surface plasmon resonance (SPR) which depends on the nanoparticle size and includes the contributions of the free electrons, surface damping, and interband transitions or bound electrons [23-24].

2.2 Localized surface plasmon resonance

When an external electromagnetic wave is applied to a metal, the collective conduction electrons oscillate resulting in the perturbed charge distribution, in what is known as "*plasma oscillation*". The surface plasmon resonance (SPR) is hence a collective excitation mode of the plasma localized near the metal surface.

In the case of a metal nanoparticle, the surface plasmon mode is restricted due to small dimensions to which the electrons are confined. The surface plasmon mode must conform to the boundaries of the dimensions of the nanoparticles. Therefore, the resonance frequency of the surface plasmon oscillation of the metal nanoparticles is different from the plasma frequency of the bulk metal. Surface interactions can alter the optical properties and influence the spectral profile of the light scattered by the SPR of the metal nanoparticles. Among the metal nanoparticles known to exhibit SPR, silver nanoparticles have an especially strong SPR [25].

When the incident photon frequency resonates with the collective oscillation of the conduction electron in the metal nanoparticles, the frequency is known as the *Localized Surface Plasmon Resonance* (LSPR) frequency [26]. A LSPR is generated when the size of a nanoparticle is much smaller than the wavelength of incident radiation. The LSPR is a dipolar excitation between the negatively charged electrons and the positive charge lattice in the particle as shown in Figure 2.1 [25]. The LSPR depends on the size, shape, interparticle spacing and dielectric properties of the material, as well as the dielectric properties of the local environment around the nanoparticles. The LSPR extinction maximum (λ_{max}) of the nanoparticles can be measured by UV-Visible spectroscopy.
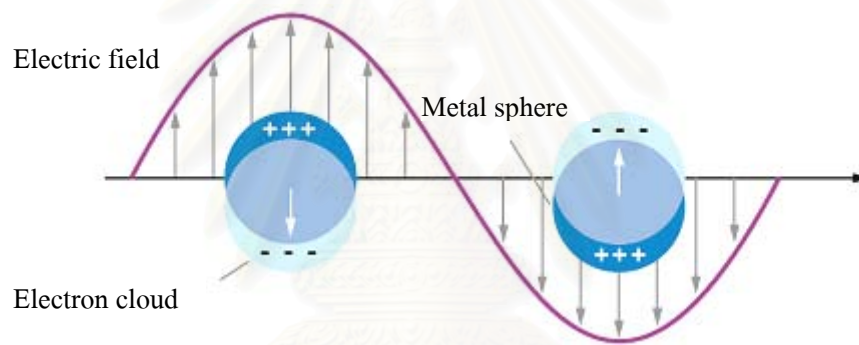
Figure 2.1   Schematic diagrams of LSPR [25].

2.2.1   Small nanoparticles versus large nanoparticles

For spherical nanoparticles, the absorption and scattering depend on the particle size. The nanoparticles with less than 40 nm diameter the scattering are negligible, and the particles only absorb energy. On the other hand, nanoparticles with 40 nm and larger, scattering becomes very important. The colors of nanoparticles occurred from strongly absorption and scattering, but the color of small particles is mainly caused by absorption.

Small particles (< 40 nm)

When the size of nanoparticle is much smaller than the wavelength of the incident light, the nanoparticles feel a field spatially constant, but with a time dependent phase, which is known as *the quasi-static limit*. The absorption energy of nanoparticles through the following mechanisms: (1) collective excitations of the free electron leads to surface plasmon resonance. (2) interband transitions which electron transitions from occupied to empty bulk bands. The electrons are bound by a restoring force given by the energy difference between ground and excited electronic states, usually at the ultraviolet region. (3) Surface dispersion of the free electrons. The charges are done homogenously, gaining a dipolar charge distribution on the surface.

Large particles (> 40 nm)

For the size of the nanoparticles are above 40 nm, the radiation effects become more important. The displacement of the electronic cloud is no longer homogeneous. The high multipolar charge distributions are induced. This fact can be described Mie theory. The ratio between the size of the particle and the wavelength of the incident light has the effect to the accelerated electrons. The electrons lose energy experiencing a damping effect due to secondary radiation. It makes wider the SPR. This field reacts against the quasi-static polarization field and shifts the position of the modes to larger wavelengths. Thus, the radiation damping reduces the intensity and makes broader and asymmetric the SPR peaks, which are red-shifted [23]. The damping mechanism is shown in Figure 2.2.
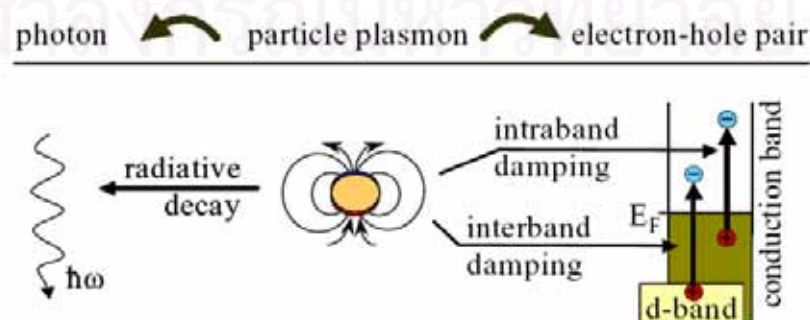
Figure 2.2   Schematic diagrams of damping mechanism of particle plasmon

2.3 Synthesis of silver nanoparticles

For metal nanoparticles, their physical and chemical properties are dependent of their size and shape. Thus, controlling the morphology and size of nanoparticles are important which achieved by varying stabilizer, reducing agent and all the conditions. Currently, the various methods of synthesis nanoparticles are explored.

2.3.1 Physical methods

The preparations of metal nanoparticles by physical methods are many different methods. Physical methods are the methods which employ low-temperature plasma, molecular beams, gas evaporation, cathode sputtering, shock wave, electroexplosion, laser-induced electrodispersion, supersonic jets, and different versions of mechanical dispersion. The approaches of these methods are produced from large structure to small structure. The major methods are based on combining metal evaporation into an inert gas flow with the subsequent condensation in a chamber maintained at a certain temperature [27].
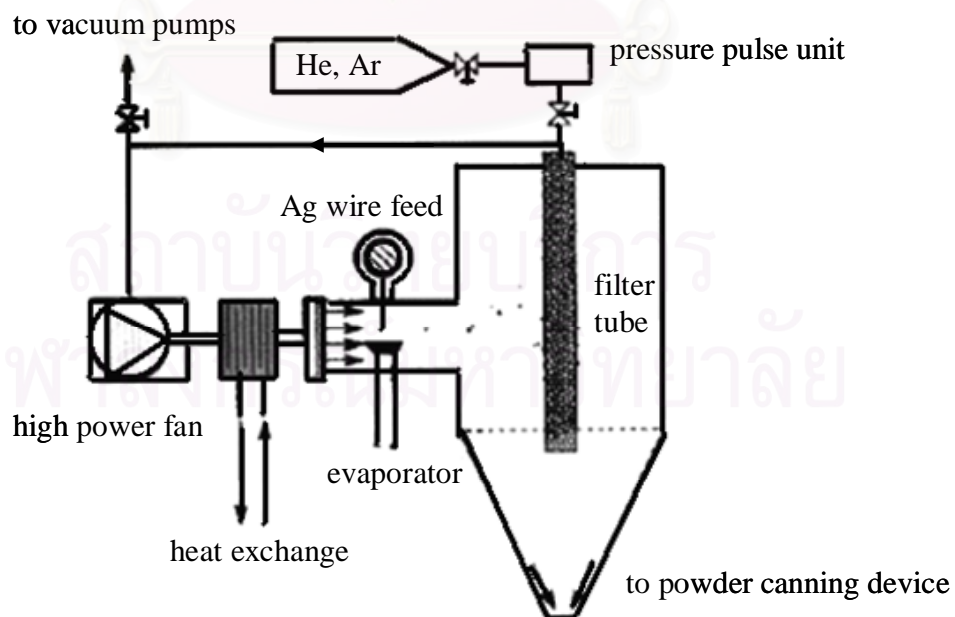
Figure 2.3   Schematic diagrams for the preparation of silver nanoparticles by inert gas condensation method [27].

2.3.2   Chemical methods

Nowadays, many scientists and researchers are interested in the development of modern and new methods for synthesis and stabilization of metal nanoparticles. In addition, the method can be synthesized the desire silver nanoparticles in shape and size. Chemical reduction is one method to use most widely in the liquid phase, including aqueous and nonaqueous media. Chemical method is the simple method which can easily adjust the experimental parameters.

Metal compounds including metal salts are reduced by aluminohydrides, borohydrides, hypophosphites, formaldehyde, citrate and salts of oxalic and tartaric acids as the reducing agent. Some reducing agents are both the reducer and the stabilizer. Generally, the behavior of a metal particle in solution is determined by the potential difference [27]:

$$\Delta E \;=\; E - E_{redox} \hspace{4cm} 2.9$$

where E is the equilibrium redox potential of the particle and E_{redox} is the corresponding solution potential. Particles grow when $\Delta E > 0$ and dissolve when $\Delta E < 0$. For $\Delta E = 0$, an unstable equilibrium is established.

The redox potential of metal nanoparticles is complicated due to it depends on the number of atoms. Chemical reduction is a multifactor process. Furthermore, the redox reaction are also depends on the choice of a redox pair and concentration of its components as well as on the temperature, pH of the medium, diffusion and characteristics and environmental of experiment.

Borohydride reduction

Strong reducing agent most frequently used in the reduction of metal ions can produce small particles and monodisperse. The reaction is fast and can be scaled up to large scale synthesis. The strong reducing agents are tetrahydroborates of alkali metals (MBH_4), which were operated in acidic, neutral, and alkaline aqueous media.

Alkali-metal tetraborates can reduce most cations of transition and heavy metals, which is explained by the high redox potential of MBH_4 (1.24V in alkaline medium) as compared with the standard potentials of many metal ions, which lie in the $-0.5 \leq -E \geq = -1.0V$.

The mechanism of reduction of metal ions with alkali-metal tetraborates was explained. It involves the formation of complexes with bridge bonds M---H---B. After that the subsequent hydrogen-atom transfer favors to break the bridge bonds which metal atom is released. And reaction followed by a redox process with the breakage of a B-H bond to give BH_3. Chemical interactions in the reduced-metal-ion-reducer system can be associated with the transfer electron from reducer to metal ion via the formation of an intermediate complex. Intermediate complex have lowers the electron-transfer energy [27].

Preparation of small particle size of silver sols can be prepared with sodium borohydride reduction [28]. Small particles or seed was used as nuclei for preparation of larger particles.

2.4 Immobilization of silver nanoparticles on materials

In textiles application, engineering of silver nanoparticles are becoming increasingly to manufacture of clothing, underwear and socks. Silver nanoparticles coating are more widespread due to their strong antibacterial property. The method for immobilization them on material is "***padding process***" because it is easy and of low cost.

2.4.1 Padding process

In general, fabric padding is one of textile dyeing process. This process was developed by Beautech Ltd., Rock Hill, South Carolina in United States. Pad batch dyeing is a more environmentally-sound and high quality dyeing method. It is simple, versatile, and flexible without major capital investment in equipment. Furthermore, pad batch dyeing offers several significant advantages such as cost and waste reduction resulting to waste water treatment cost, over other conventional dyeing process.

The basic technique in padding process is to saturate the prepared fabrics with pre-mixed dye solution. After that, the fabric is run through rollers. The rollers are also called padder. The padders force the dye into the fabric with the process while removing excess dye solution. The padding process is shown in Figure 2.4
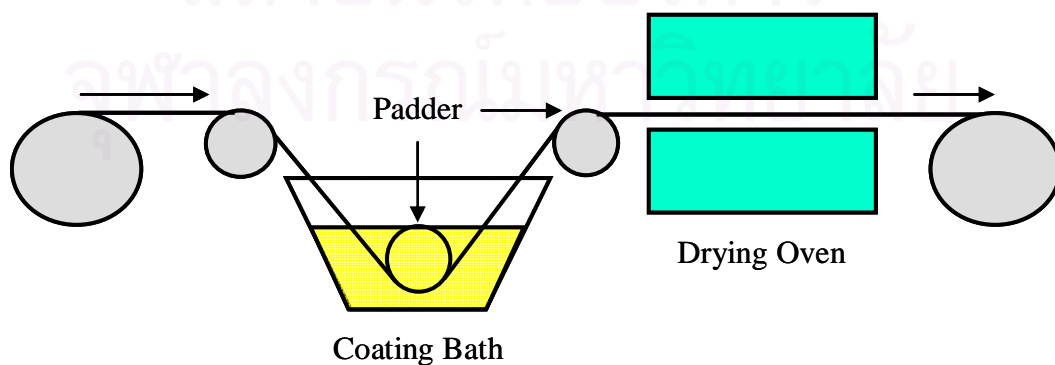
Figure 2.4   Padding process including coating bath, padder, and drying oven

The fabric that undergoes the padding process retains a smooth, uniformly colored appearance with added luster and a soft touch and wearing. It is also brighter in shade and has a better look and feel [29]. Additionally, the quality of the fabric can be improved in this process. For example, the antibacterial agents or softeners can be applied due to no change process or equipment. This method prefers the textile industry for large scale production.

2.5 Application of silver nanoparticles

For novel phenomena and properties of silver nanoparticles, the fabrication of silver nanoparticles is investigated. The applications have found in many different fields of science.

2.5.1 Silver nanoparticles as a conductive ink and paste

Silver nanoparticle has a high conductivity due to high surface area. Silver nanoparticles exhibit a drastic decrease in melting point so silver nanoparticles is one of the suitable substances to achieve conductive inks and pastes. This is applied to electronic devices. Many researchers studied and prepared silver nanoparticles for conductive ink and paste.

Magdassi et. al. [30], prepared and characterized stabilized concentrated silver nanoparticles colloid that can be used as a pigment in ink-jet inks. Carboxylmethyl cellulose (CMC) was used as both stabilizer and binder. Conventional pigments in ink-jet inks contain particles in the size range of 100-400 nm. The particle sizes are about 50 nm or less improve image quality and print head reliability. The nanoparticles were prepared by reducing silver nitrate with trisodium citrate with 0.2 wt% of CMC. For preparing the high silver nanoparticles concentration, the 0.1 %wt CMC-stabilized silver nanoparticles were lyophilized to reduce the water content or remove the total water content. The silver powder was redispersed in a proper amount of water. The particles size are about 40-70 nm. After storage at ambient temperature

for 7 months, the particles size increases only up to 90-120 nm. Silver nanoparticles in this process were shown to be suitable as pigments in water-base ink-jet inks.
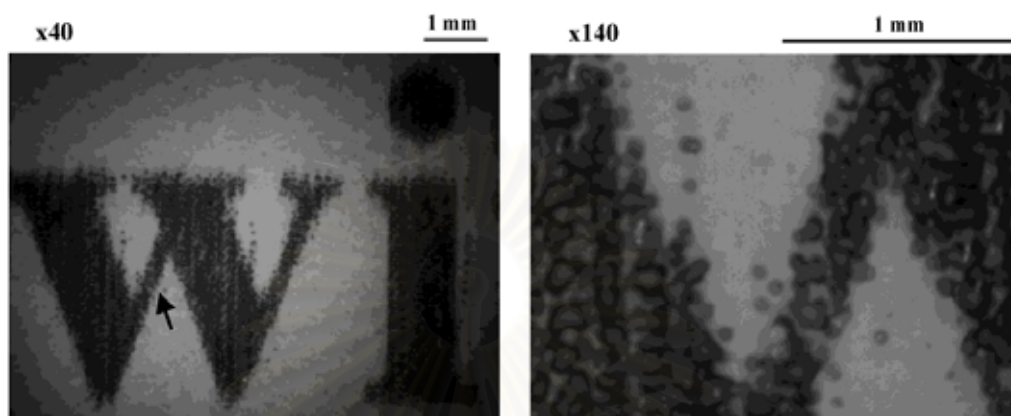
Figure 2.5   Image (magification×40 and ×140) printed on ink-jet transparency with the use of the ink formulation contains 1 wt% of silver, 0.2 wt% of CMC, and surfactants.

2.5.2 Silver nanoparticles as a sensor

Silver nanoparticles exhibit a phenomenon known as a surface-enhanced Raman scattering (SERS) in which the Raman scattering cross sections are dramatically enhanced for the molecules adsorbed thereon.

Kim et al. [31] demonstrated that an invaluable tool for multiplex biomolecular sensing and recognition via SERS and SERRS by using 2-µm-sized Ag powder as a core material and rhodamine B isothiocyanate (RhBITC) as a SERRS maker molecules. The basic strategy is schematically presented in Figure 2.6.
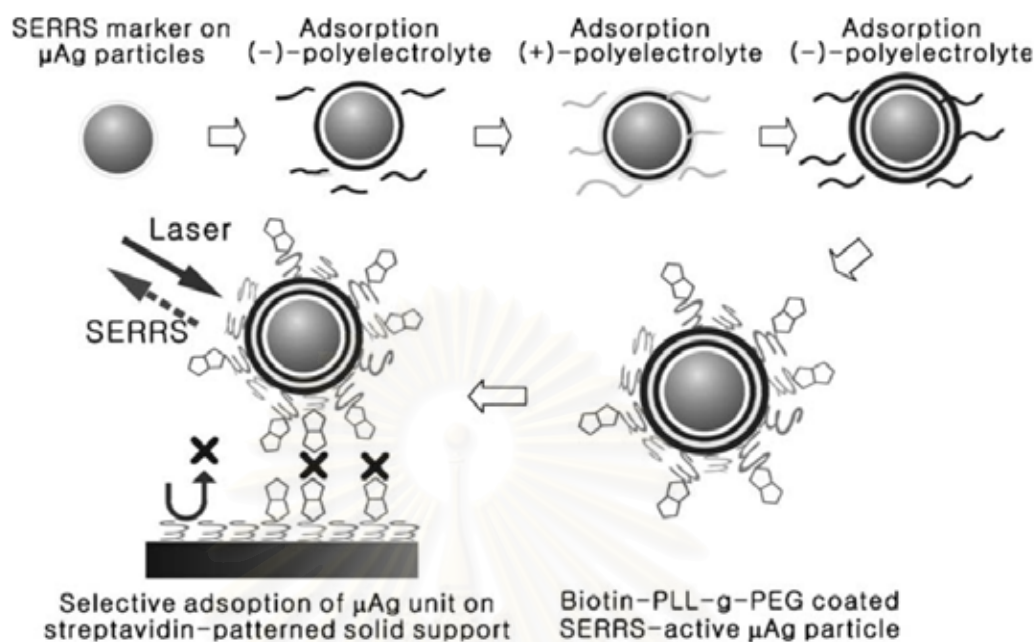
Figure 2.6   Schematic diagrams of fabrication of 2-μm-sized Ag particle-based surface-enchanced resonance Raman scattering (SERRS) unit for ready application to biomolecular sensing and recognition. PLL poly(L-lysine), PEG poly (ethylene glycol).

RhBITC was adsorbed initially on μAg powder. Then poly(acrylic acid) (PAA) and poly(allylamine hydrochloride) (PAH) were deposited on the Ag powders. The outermost PAA layer of the powders bound biotinylated-PLL-g-PEG. Those μAg particles were finally interacted with strepavidin arrays formed on a separate biotinylated glass slide and were measured by Raman spectroscopy. Strepavidin was varied concentration to figure out the detection limit of the μm-Ag-based sensing units.

They evaluated that SERRS spectra were obtained as a function of the strepavidin concentration. At strepavidin concentration above 10^{-9} g mL^{-1}, SERRS spectrum were very intense while the concentration of strepavidin was 10^{-10} g mL^{-1}, SERRS intensity decreased. It showed that the number of Ag particles adsorbed on the biotinylated substrates decreased. This clearly illustrated the usefulness of μAg

particles as a core material for fabricating in a very simple way that highly effective biomolecular sensing/recognition units are operating via SERS-SERRS.

2.5.3   Silver nanoparticles as an antibacterial agent

Long time ago, silver has been employed to control microorganisms and fight inflections. The ancient people used silver in drinking water for inhibition the growth of bacteria. So the antibacterial and anti-viral actions of silver nanoparticles, silver ions have been thoroughly investigated.

Lee et. al. [32], investigated the antibacterial efficacy of nanosized silver colloidal on the cellulosic and synthetic fabrics against *S. aureus* and *K. pneumoniae*. The silver particles size was 2-5 nm which was dispersed on the fabrics. Cotton and polyester were padded through 25 ppm and 50 ppm silver colloids. In Figure 2.7, SEM images show the silver nanoparticles on cotton and polyester. The silver nanoparticles are well dispersed on the each fiber surface. They were investigated the antibacterial effect after laundering fabrics at 5 cycles, 10 cycles, and 20 cycles washing. It was found that after 20 washing the cotton and polyester showed excellent antibacterial efficacy against *S. aureus* and *K. pneumoniae*.
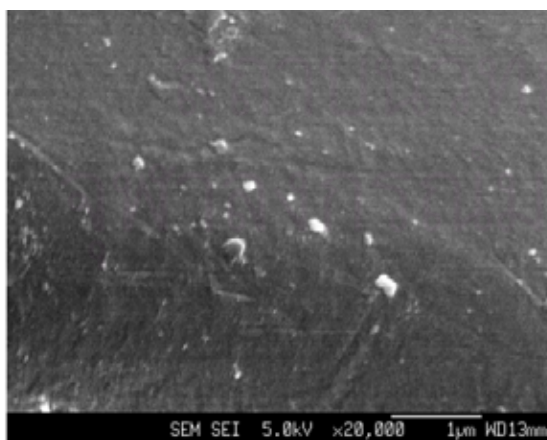
A : Cotton   B : Polyester
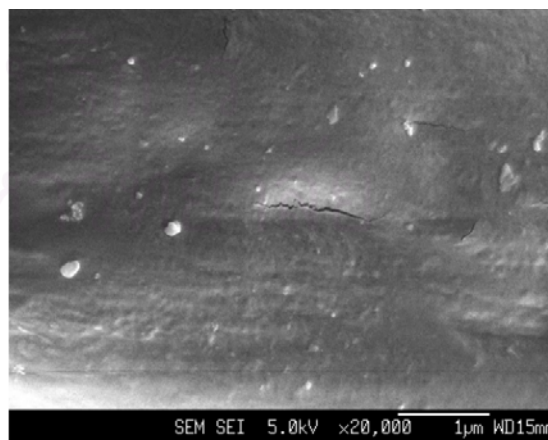
Figure 2.7   SEM images of nano-particles on cotton (A), and polyester (B).

2.6 Antibacterial property of silver nanoparticles

Silver nanoparticles (AgNPs) and silver compounds have long been known to exhibit a strong toxicity to microorganisms as many as 650 species of bacteria [33]. Resistant bacteria to silver nanoparticles are rare strains comparing with the antibiotics.

Biocides (such as silver ions or silver nanoparticles) and antibiotics have differing modes of action [34].

1. Biocides (such as silver ions or silver nanoparticles) have multiple target sites on or within bacterial cells and have broad activity to act to bacteria.

2. Antibiotics have specific target sites on or within a bacterial cell and have a narrower spectrum of activity resulting in the bacteria would develop a host mutation simultaneously to protect itself.

Several reports demonstrated that the surface of the bacteria corresponds with the size and the faceting of the particles especially the directing interaction of the {111} facets. Pal and coworkers [17] found that truncated triangular silver nanoplates with a {111} facet displayed high the antibacterial activity. From the result of Morones et al [33], showing that the average size of the nanoparticles is about 5 nm with a standard deviation of 2 nm are only penetrating into the bacteria and directly interact with the membrane. It illustrated that the antibacterial property of silver nanoparticles are size dependent. Smaller particles having the larger surface area will give more bactericidal activity than the larger particles for interaction with bacteria.

The mechanism of the bactericidal effect of silver nanoparticles against bacteria is not very well-known. From experimental evidence of many studies illustrate that silver nanoparticles showed the bactericidal activity in three ways [33, 34].

1. Nanoparticles attach to the surface of the cell membrane if the size of particles is in the range of 1-10 nm and drastically disturb its proper function, like permeability and respiration.

2. Silver nanoparticles are able to penetrate inside the bacteria and damage the bacteria cell by interacting with sulfur and phosphorus containing compounds such as DNA which affect bacteria in processes such as respiratory chain and cell division.

3. Nanoparticles release silver ions from the particles, which interacted with thiol, sulphydryl, amino, imidazole, phosphate and carboxyl groups of membrane or enzyme proteins that leading to protein denaturation.

2.7 Cytotoxicity of silver nanoparticles on human body

The use of silver nanoparticles becomes more and widespread in various applications such as medical and healthcare, textiles, or paint. Although silver nanoparticles are widely used in modern technology, there are a few studies about information concerning the human health after entering via different portals. The toxicity of silver nanoparticles is greater than that of bulk silver. Due to extra small size of silver, they are greater mobile in both the human body and the environment.

The United Stated Food and Drug Administration (FDA) has warned as early as 1999 that the "use of colloidal silver solutions has resulted in cases of argyria, a permanent blue-grey discoloration of the skin and deep tissues" [35].

In case report [36], a 58-year-old man was referred argyria or cutaneous discoloration after he drank colloidal silver protein solution for at least 1 year but was unable to estimate his total consumption. The skin was a deep blue/grey especially sun-exposed sites such as the face, the 'V' of the neck, the bald scalp, the hands and the forearms. The mechanism of silver deposition in agryria is not well-known. Silver was form silver-protein complexes by reducing to silver sulphide and selenide in the

skin. This process was catalyzed by sunlight. They combined with melanocyte stimulation and caused the cutaneous discoloration. Argyria was used to treat by hydroquinone and dermabrasion but both were unhelpful. Furthermore, laser techniques were unhelpful too. Generalized argyria seldom affect to the systemic problems except for the social humiliation caused by the discoloration.

In comparison, *In vitro* (test tube) studies demonstrate that nanosilver is toxic to mammalian liver cells [37] and stem cells [38]. BRL 3A rat liver cells were used to test cytotoxicity of metals nanoparticles such as silver, molybdenum, iron oxide, titanium dioxide and aluminum. The results showed that silver nanoparticles were the most toxic nanoparticles. Silver added to the cells to reduced drastically mitochondrial functions and cell viability.

In some recent studies revealed that nanoparticles of various chemical compositions could be induced oxidative stress in lung epithelial cells. The phagocytic function of alveolar macrophages was impaired resulting in building up a toxic dose which may sustain inflammation [39]. In addition, the lungs have protected mechanisms to eliminate inhaled solid particles so that particle deposition is not sufficient to achieve respiratory pathogenic effects.

Coadiovascular events such as coagulation and cardiac rhythm disturbances of rats were examined the pulmonary and systemic distribution after inhalation and implantation ultrafine silver particles (14.6±1.0 nm) [38]. The result showed that the silver content in the lung decreases rapidly with time. Subsequently, they detected ultrafine silver particles in blood and other organs such as heart, liver, kidney, and even brain in rats. They mentioned that the most portion of silver was observed in the liver. This indicates that liver might play a prime role in clearance of circulatory silver nanoparticles.

Silver bone cement was tested with mouse fibroblasts and human osteoblasts in vitro by the release of lactate dehydrogenase (LDH assay), total protein content, and

number of vital cell [40]. The result showed that silver bone cement was not toxic. The animal cells are eukaryotic cells which have a strong stratum structural which contrast to the bacteria cell which was prokaryotic cell.

Yet, the cytotoxicity of silver nanoparticles on human body has yet to be clarified. So the effect of silver nanoparticles on human health should be investigated before silver nanoparticles boom.

CHAPTER III

EXPERIMENTAL   SECTION

The stable and highly concentrated colloidal silver nanoparticles were synthesized by reduction method in the presence of stabilizer. Gelatin, PVP, and starch were used as stabilizer for controlling the size, shape, size distribution, and stability of silver nanoparticles. Their stability efficiencies were compared. Silver nanoparticles synthesized in the presence of the best stabilizer were immobilized on cotton and polyester by padding process. The immobilization of silver nanoparticles on the fabrics and antibacterial properties were studied.

3.1   Material and chemicals

Silver nitrate ($AgNO_3$, 99.99%, Analytical Grade) was purchased from Fisher Scientific UK Limited, Thailand. Sodium borohydride ($NaBH_4$, guarantee for analysis), starch (amylum, potato starch for determination of diastase, guarantee grade for analysis), gelatin, and poly(vinyl pyrrolidone) (PVP) were obtained from Merck, Thailand. These were used without any further purification. Deionized water (DI) was used in the preparation of all samples. Padding operation including coating, padding, and drying were performed at Nan Yang Inspiration Center Co., Ltd., Kratoombean, Samutsakorn, Thailand. Cotton and polyester fabrics were provided by Nan Yang Textile Group. The silver nanoparticles immobilized were tested against *Staphylococcus aureus* (*S. aureus*), a Gram-positive bacterium for their antibacterial properties by AATCC test method 147-1998 of the American Association of Textiles Chemist and Colorists.

3.2 Instruments

3.2.1 Ocean Optics UV-Visible portable spectrometer

Ocean Optics UV-Visible portable spectrometer was set as shown in Figure 3.1. The light source and ocean optics USB4000 spectrometer were attached with the fiber optic. The optical spectra were obtained with a standard deuterium lamp (thorlabs, 150 w) and a fiber coupled spectrometer (ocean Optics, 350-1100 nm). The plasmon extinction spectra from collecting by UV-Visible spectrometer show the preliminary size, shape, and size distribution of silver nanoparticles.

Instrumental Setup

Model	USB4000
Source	Deuterium-Halogen light source DH 2000
Wavelength range	UV-Vis-NIR
Detector	Toshiba TCD1304AP, 3648-element linear silicon CCD array
Grating	600 Line Blazed at 300 nm
Bandwidth	200-850 nm

Spectral Acquisition Parameters

Software	Ocean Optics Inc. Spectra Suite
Integration time	10 milliseconds
Scans to Average	128 scans
Box car width	10 nm
Spectral format	Absorbance
Spectral range	200-850 nm

Figure 3.1   Ocean Optics UV/Visible portable spectrometer (USB 4000, Toshiba TCD 1304AP).

3.2.2 Electron microscope

3.2.2.1   Scanning electron microscope (SEM)

The SEM images were obtained by using a JEOL, JSM-6480LV with accelerating voltage of 10 kV as shown in Figure 3.2. This was used to study immobilization of silver nanoparticles on the fabrics.

Figure 3.2   Scanning electron microscope (JEOL, JSM-6480LV, Japan).

3.2.2.2   Transmission electron microscope (TEM)

The TEM images were captured on Hitachi, H-7650 operated at an accelerating voltage of 100 kV as shown in Figure 3.3. The TEM images show the size, shape, and size distribution of silver nanoparticles to confirm the result from Ocean Optics UV/Visible portable spectrometer.

Figure 3.3   Transmission electron microscope (H-7650 Hitachi, from Japan).

3.2.3   Padder

Padder [Shanghai Colorpilot Electron Co., China on Rapid brand (Model P-AO)] in padding process was performed at Nan Yang Inspiration Center Co., Ltd., Kratoombean, Samutsakorn, Thailand. The wet pick-up ratio can be adjusted by controlling the pressure of padder.   In this experiment, padder was operated at pressure of 3.0 bars for 80 % of the wet pick-up ratio as shown in Figure 3.4.

Figure 3.4   Padder (Model P-AO on Rapid brand from Shanghai Colorpilot Electron Co., China).

3.2.4 Mini dryer

Mini dryer [Shanghai Colorpilot Electron Co., China on Rapid brand (model R-3)] at Nan Yang Inspiration Center Co., Ltd., Kratoombean, Samutsakorn, Thailand used to dry fabrics after the fabrics passing through padder. Drying temperature and time of mini dryer can be adjusted. The temperature can be adjusted in the range of 20 °C – 250 °C. The largest sample size is about 36×42 cm^2. In this experiment, the fabrics size was 10×42 cm^2. Mini dryer was operated at 150°C and controlled the time for 90 seconds as shown in Figure 3.5.

Figure 3.5   Mini dryer (Model R-3, Rapid brand, Shanghai Colorpilot Electron Co., China).

3.3 Preparation of stabilizers solution

Gelatin, PVP, and starch were used as stabilizer in the synthesis of silver nanoparticles. The concentrations of each stabilizers solution were 2 wt% (2 g/100 mL). In a typical preparation, 2 g of gelatin was dissolved in 100 mL deionized water and stirred for 30 min at 50°C. The solution was filtered through Whatman No.1 filter paper to remove insoluble substances. PVP and starch solution were prepared with the same procedure as that of gelatin solution except that PVP was dissolved at room temperature and starch was heated at 80-90 °C.

3.4 Synthesis of silver nanoparticles by the reduction method in the presence of stabilizer

In the presence of gelatin solution, 10,000 ppm silver nanoparticles were synthesized by the reduction of $AgNO_3$ with $NaBH_4$. The silver salt solution was prepared by dissolving 1.6 g of $AgNO_3$ in 10 mL deionized water and then added 20 mL gelatin solution into the $AgNO_3$ solution. The reducing agent was prepared by dissolving 0.25 g of $NaBH_4$ in 10 mL deionized water and 60 mL gelatin solution was added into $NaBH_4$ solution. Ag^+ was reduced by the injection of $AgNO_3$ solution into $NaBH_4$ solution with vigorous stirring. The color of the solution became brown because the silver nanoparticles were generated. Vigorous stirring was maintained throughout the entire synthesis for 1 hour. All steps were performed at room temperature. The procedures of the synthesis silver nanoparticles in the presence of PVP and starch are the same as that of the silver nanoparticles with gelatin**.**

3.5 Characterization of silver nanoparticles in the presence various stabilizers

The size, shape, and size distribution of the synthesized silver nanoparticles in the presence of various stabilizers were characterized by UV-Visible spectroscopy and TEM. For UV-Visible analysis, 10,000 ppm of colloidal silver nanoparticles were diluted in deionized water into 10 ppm, 7 ppm, 5ppm, 3 ppm, and 1 ppm. The plasmon extinction spectra implied the preliminary size, shape, and size distributions

of silver nanoparticles. All plasmon extinction spectra were recorded at room temperature in quartz cuvettes (1 cm optical path). Before collecting the plasmon extinction spectra of the synthesized silver nanoparticles, deionized water was analyzed as a blank sample.

The samples for TEM study were prepared by placing a small drop of the testing solution onto a formvar-covered copper. The solvent was allowed to evaporate at room temperature for 24 hours. The TEM images were captured via a Hitachi, H-7650 operated at an accelerating voltage of 100 kV which showing size, shape, and size distribution of silver nanoparticles.

3.6   Stability of silver nanoparticles in the presence of various stabilizers

The synthesized silver nanoparticles in the presence of various stabilizers were kept for 3 months at ambient condition. The size, shape, and size distributions of these silver nanoparticles were measured by Ocean Optics portable UV-Visible spectrometer and TEM. The most stable silver nanoparticles with the smallest size was used to immobilize on the fabrics and studied for antibacterial properties.

3.7   Padding of silver nanoparticles on cotton and polyester fabrics

The colliods containing the smallest silver nanoparticles with a narrow size distribution and high stabilization were used in this process. The concentration of colloidal silver nanoparticles was varied. The 10,000 ppm colloidal silver nanoparticles were diluted to 12.5 ppm, 25 ppm, 62.5 ppm, 125 ppm, and 250 ppm. The wet pick-up ratio of cotton and polyester fabrics was 80 %. The real concentrations of silver nanoparticles on the fabrics were estimated from Equations (3.1) and (3.2).

$$\text{Wet pick-up ratio (\%)} \quad = \frac{\text{wet weight - dry weight}}{\text{dry weight}} \times 100 \qquad (3.1)$$

where wet weight and dry weight are the weight of silver-coated cotton or polyester fabrics after padding and the weight of cotton or polyester fabrics, respectively [41].

$$C_2 = \frac{C_1(\text{wet weight - dry weight})}{\text{dry weight}} \qquad (3.2)$$

where C_1 and C_2 are concentration of colloidal silver nanoparticles and concentration of silver nanoparticles on cotton or polyester fabrics, respectively.

From Equations (3.1) and (3.2), the real concentration of silver nanoparticles on cotton and polyester fabrics were controlled to be 10 ppm, 20 ppm, 50 ppm, 100 ppm, and 200 ppm. The cottons and polyester fabrics were cut into pieces with dimension of 10×15 cm^2. Cottons fabrics were padded through the silver solution bath with each concentration of colloidal silver nanoparticles solution and passed through the padder at the pressure of 3.0 bars as shown in Figure 3.6 (A). After padding, cottons fabrics were immediately dried in mini dryer at 150°C for 90 seconds as shown in Figure 3.6 (B). The procedures of padding of polyester fabrics are the same as that of cottons fabrics.

| A: | Silver-coated cotton fabric was passed through padder. | B: | Silver-coated cotton fabric in were dried mini dryer. |

Figure 3.6   Padding process.

3.8   Antibacterial test of silver nanoparticles on cotton and polyester fabrics

To confirm the immobilization of silver nanoparticles, the antibacterial properties of fabrics sample were tested against a Gram-positive bacterium, *Staphylococcus aureus* (*S. aureus*) by AATCC test method 147-1998 of the American Association of Textiles Chemist and Colorists. The 20 and 50 ppm of silver nanoparticles-coated cotton and polyester fabrics were used. The fabrics were washed for 20 times before antibacterial test. The bacteria culture was streaked onto the clear nutrient agar medium in each dish. Then the piece of blank and silver nanoparticles-coated fabrics samples were placed directly on top of streaks in the nutrient. The dishes were then incubated for 24 hours at 37°C. After incubation, the plates were examined for the inhibition of growth underneath and near the edge of the test fabrics along each streak of inoculums. The antibacterial efficacies of both samples were studied.

3.9   Characterization of silver-coated cotton and polyester fabrics by SEM

The 20 times washing of 20 and 50 ppm silver-coated cotton and polyester fabrics were characterized by SEM. The samples for SEM study were prepared by cutting silver-coated cotton and polyester fabrics with each concentration by dimension of 0.5×0.5 cm^2. The SEM images were captured by a JEOL, JSM-6480LV with accelerating voltage of 10 kV. All samples were placed on grid, sputter-coated with thin gold, and placed in sample chamber.

CHAPTER IV

RESULTS AND DISCUSSION

This chapter is divided into three sections. The first section showed the results of the synthesis and characterization of silver nanoparticles with various stabilizers. Three types of stabilizer were used as well as gelatin, PVP, and starch. The stability of silver nanoparticles with these stabilizers were observed. The second section was to investigate the immobilization of silver nanoparticles on cotton and polyester. And the last section showed the antibacterial test of silver nanoparticles on the fabrics.

4.1   Synthesis of silver nanoparticles with gelatin as a stabilizer

In the synthesis of 10,000 ppm colloidal silver nanoparticles with gelatin as a stabilizer by reduction method, it was observed that the color changed immediately when the first drop of $NaBH_4$ was added, showing the formation of silver nanoparticles. Finally, the solution turned into dark brown color as shown in Figure 4.1. For testing the completeness of the reaction, NaCl was added into the synthesized silver nanoparticles to test for Ag^+. If Ag^+ remains in the reaction, it reacts with Cl^- to from AgCl(s). After adding NaCl, there was no precipitation of AgCl. It showed that this redox reaction was completed. The redox reaction can be written as follows [41]:

Reduction: $2Ag^+ + 2e^- \longrightarrow 2Ag^0$

Oxidation: $2BH_4^- + 6H_2O \longrightarrow 2H_3BO_3 + 7H_2 + 2e^-$

Redox: $2AgNO_3 + 2NaBH_4 + 6H_2O \longrightarrow 2Ag + 2NaNO_3 + 2H_3BO_3 + 7H_2$
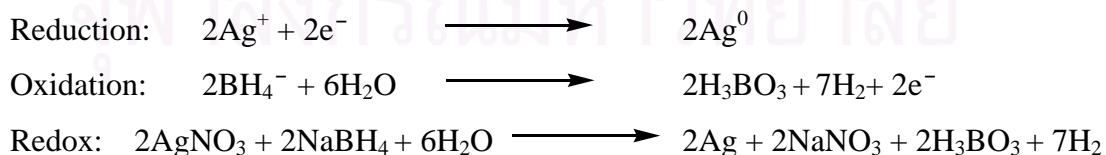
Figure 4.1   The synthesized silver nanoparticles with gelatin as a stabilizer: highly
               concentration (10,000 ppm) of silver nanoparticles.

**4.1.1   Characterization of silver nanoparticles with gelatin as a stabilizer
          by Ocean Optics UV-Visible portable spectrometer**

        To confirm that the spectra of the precursors would not affect the spectrum of
silver nanoparticles, all chemicals and precursors of silver nanoparticles synthesis
were characterized by UV-Visible spectroscopy. Figure 4.2 shows the spectra of the
precursors. Figure 4.2 (A) is the spectra of silver nitrate which shows maximum
absorption band at 300 nm of silver nitrate solution. $NaBH_4$ solution does not show
any absorption in UV-Visible region as shown in Figure 4.2 (B). The results in Figure
4.2 (C, D, and E) are the spectra of 2 wt% gelatin, $AgNO_3$ + 2 wt% gelatin, and
$NaBH_4$ + 2 wt% gelatin, respectively. All spectra show the characteristics of gelatin.
It showed that the spectra of the precursors did not overlap the spectrum of the
synthesized silver nanoparticles.
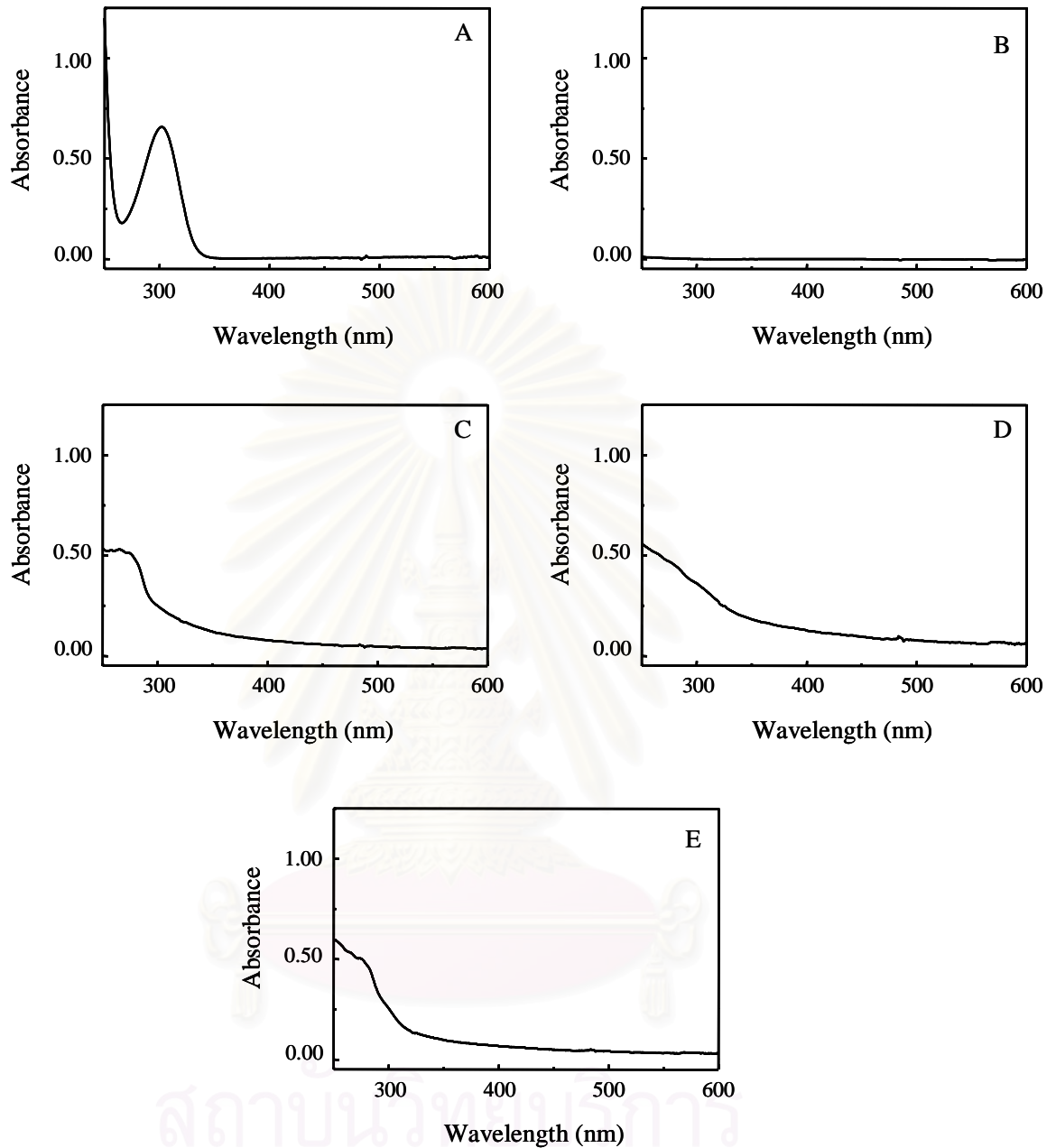
Figure 4.2   Absorption band of the precursors: the AgNO$_3$ solution (A), NaBH$_4$ solution (B), 2 wt% gelatin (C), AgNO$_3$ + 2 wt% gelatin (D), and NaBH$_4$ + 2 wt% gelatin (E).

10 ppm 7 ppm 5 ppm 3 ppm 1 ppm

Figure 4.3 Appearance of various concentrations (10 ppm, 7 ppm, 5 ppm, 3 ppm, and 1 ppm) of silver nanoparticles with gelatin as a stabilizer.
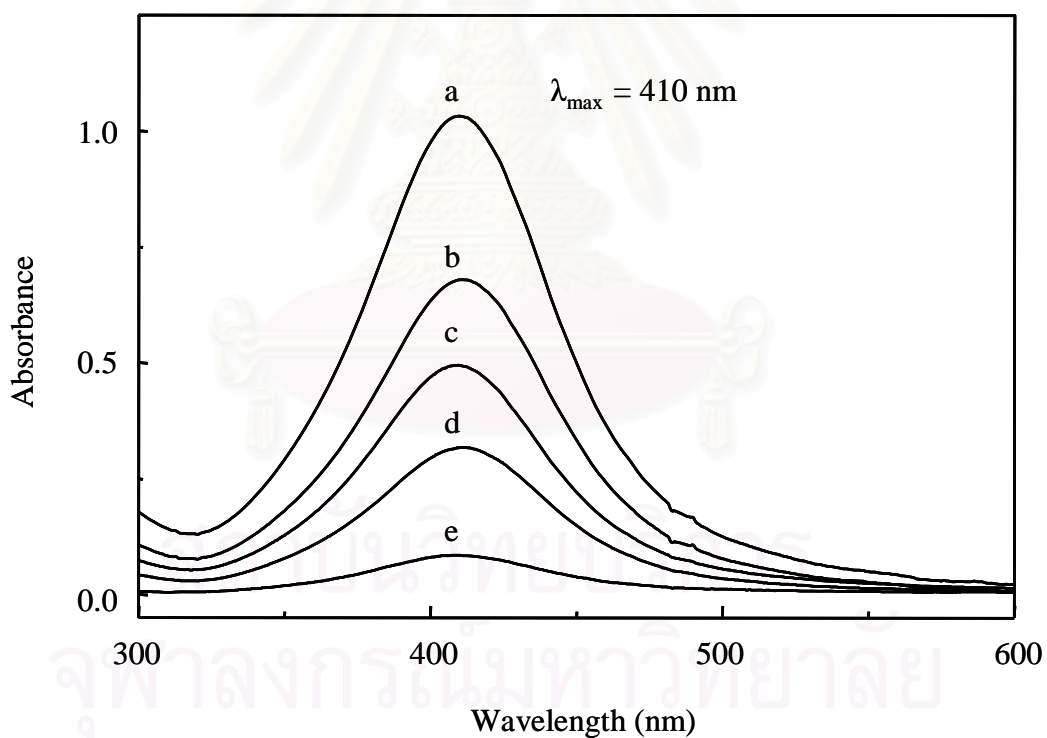
Figure 4.4 Plasmon extinction spectra of silver nanoparticles with gelatin as a stabilizer: 10 ppm (a), 7 ppm (b), 5 ppm (c), 3 ppm (d), and 1 ppm (e).

Silver nanoparticles with different concentrations (10 ppm, 7 ppm, 5 ppm, 3 ppm, and 1 ppm) had pale yellow color to yellow color as shown in Figure 4.3. From the study by UV-Visible spectroscopy, Figure 4.4 shows plasmon extinction spectra of silver nanoparticles with gelatin as a stabilizer. Plasmon spectra have a symmetrical peak with a maximum wavelength (λ_{max}) at 410 nm. It indicated that the shapes of silver nanoparticles with gelatin are rather spherical and particle sizes were rather large owing to plasmon bands shifted to the red [23]. Size distribution of silver nanoparticles was rather wide, knowing from the FWHH of spectra which was about 75 nm and corresponded to different sizs of the synthesized silver nanoparticles.

Characterization of the synthesized silver nanoparticles by UV-Visible spectroscopy is a preliminary study which cannot conclude about the quality of silver nanoparticles from plasmon extinction spectrum alone. Particles size, shape, and size distribution were subsequently studied by TEM.

4.1.2 Characterization of silver nanoparticles with gelatin as a stabilizer by TEM

TEM images of silver nanoparticles with gelatin as a stabilizer are shown in Figure 4.5 (A). The shapes of particles are rather spherical. The sizes are about 7-40 nm. The average sizes are 19.54 nm which were averaged from 200 particles and then combined into a histogram as shown in Figure 4.5 (B). The standard deviation, σ, was calculated based on the experimentally determined distributions which was 8.42 nm. The size distribution of gelatin-stabilized silver nanoparticles is polydisperse. This result is consistent with the results of the plasmon band in Figure 4.4. The mechanism of gelatin-stabilized silver nanoparticles can be explained as follows:

A
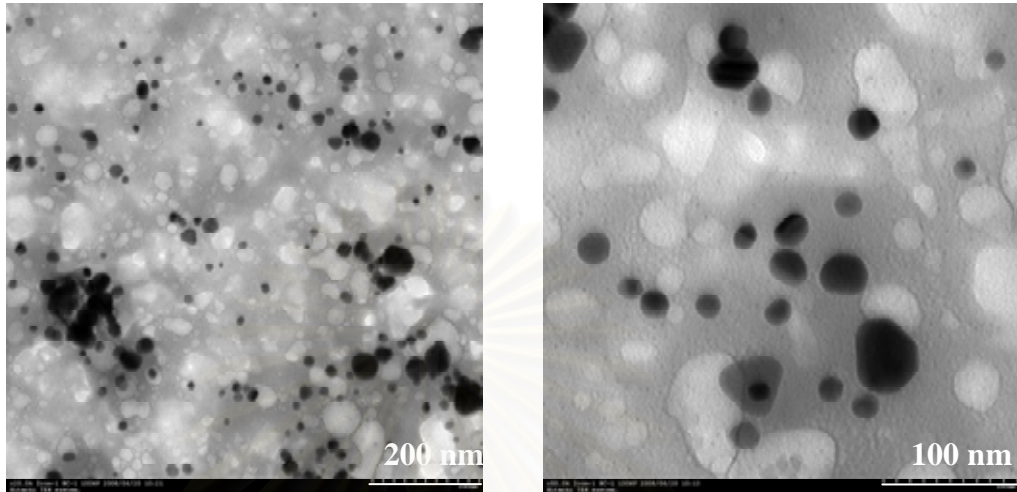
B
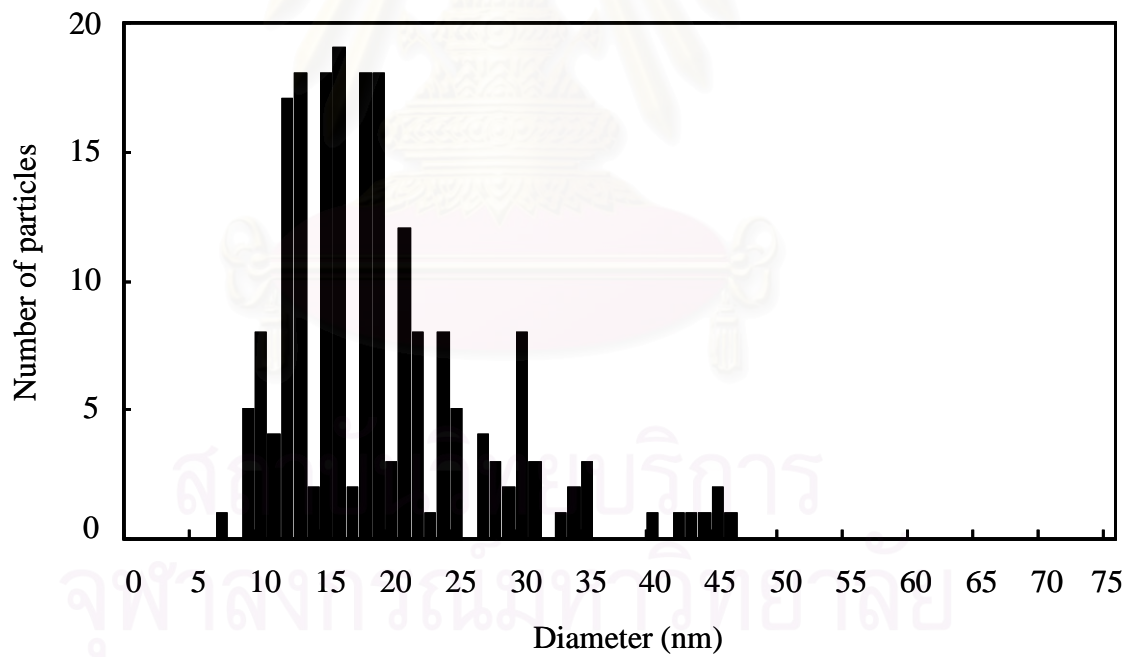
Figure 4.5   TEM images (A) and histogram (B) of the gelatin-stabilized silver
              nanoparticles.

Mechanism of gelatin-stabilized silver nanoparticles

According to literatures [43,44], the reduction and aggregation of silver ions in aqueous gelatin solutions were investigated as models for the photographic emulsion process. The effect of gelatin solution on the rate of the reduction of Ag^+ and subsequently agglomeration of silver was compared with the similar experiments in aqueous solution. The reduction of Ag^+ leads to the formation of Ag^0. The Ag^0 atoms initiated from various complexes with Ag+ ions and subsequently agglomerate to form cluster (Ag_n^+). These studies showed that Ag^+ ions bind with methionine groups in the gelatin due to lone pairs electron of sulfur to form coordinate bonds [43].

The mechanism of gelatin-stabilized of silver nanoparticles is generally proposed on the basis of its structural features. Gelatin is a biopolymer produced from partial hydrolysis of collagen extracted from animal skins, bones, tendons, ligaments. Gelatin is a mixture of single- (α), double- (β) strands gelatins, and a few triple (γ) strands polypeptides with extended left-handed helix conformations. The single (α) strand consists of 609 amino acid groups on a peptide backbone. A typical structure of amino acid in gelatin as shown in Figure 4.6 which consists of –Ala-Gly-Pro-Arg-Gly-Glu-Ser-Gly-Pro-. Amino acids of α-gelatin are shown in Table 4.1 [45]. From the structure of amino acid groups, these consist of oxygen, nitrogen and sulfur atom. Stabilization occurs when weak functional groups from any of amino acids bind with silver nanoparticles. These weakly bound functional groups can be easily exchanged with donor ligands. The steric hindrance can stabilize the silver nanoparticles.
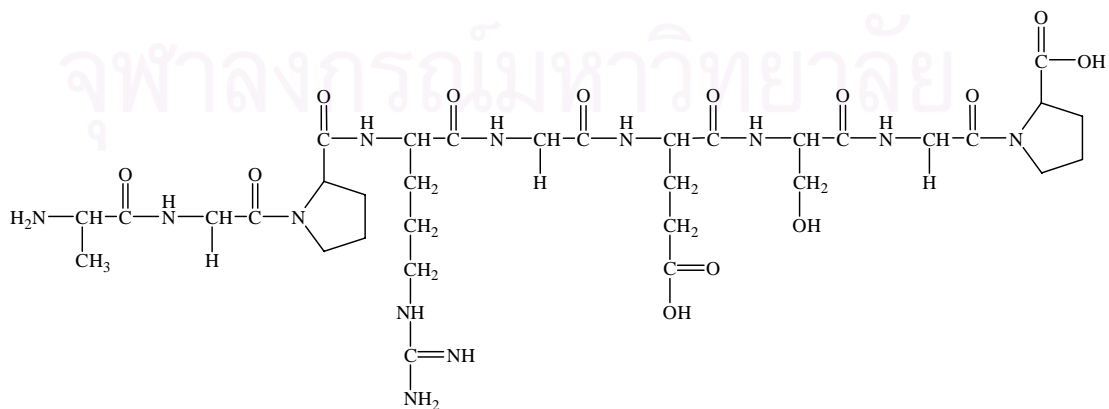
Figure 4.6   A typical structure of amino acids of gelatin.

Table 4.1   Amino acid Groups in the α-gelatin molecule [45].

Amino acid	No. per α- gelatin strand
glycine	203
proline	76
alanine	75
hydroxyproline	69
glutamic acid	33
arginine	30
aspartic acid	23
serine	20
lysine	18
valine	12
glutamine	11
luecine	11
threonine	9
phenylalanine	7
isoluecine	6
asparagine	3
methionine	2
histidine	1

4.1.3   Stability of silver nanoparticles with gelatin as a stabilizer

The stability of silver nanoparticles with gelatin was monitored. After 5 days, silver nanoparticles colloids were partially precipitated indicating that the aggregation of particles occurred. Due to amino acid groups of gelatin such as lysine, arginine, and histidine have a positive charged R groups, repulsion force of R groups with Ag^+ was occurred. Free-Ag^+ ions content in solution increased according to the increasing of the number of collisions of the molecule with the other surface silver nanoparticles. The particle size increased when keeping silver nanoparticles at room temperature for many days. It showed that gelatin is a low effective stabilizer.

4.2   Synthesis of silver nanoparticles with PVP as a stabilizer

In the synthesis of 10,000 ppm colloidal silver nanoparticles with PVP as a stabilizer by reduction method, it was observed that when the first drop of $NaBH_4$ was added, the color immediately changed into a dark brown color. It showed that the formation of silver nanoparticles occurred. At last, the solution has yellowish brown color as shown in Figure 4.7. When NaCl was added into the silver solution, no precipitation of AgCl occurred.

Figure 4.7   The synthesized silver nanoparticles with PVP as a stabilizer: highly concentration (10,000 ppm) of silver nanoparticles.

4.2.1 Characterization of silver nanoparticles with PVP as a stabilizer by Ocean Optics UV-Visible portable spectrometer

The precursors of all reaction were observed by UV-Visible spectrometer. Figure 4.8 shows the absorption band of the precursors. The result in Figure 4.8 (A) is a spectrum of silver nitrate solution which shows the maximum absorption at 300 nm. Figure 4.8 (D) is the spectrum of silver nitrate solution with 2 wt% PVP, shows the same absorption band of silver nitrate solution at 300 nm. Figure 4.8 (B), sodium borohydride solution does not show the absorption spectrum in 300-600 nm regions. Figure 4.8 (C and E) are the spectra of 2 wt% PVP and 2 wt% PVP with sodium borohydride solution, respectively. They show the little shoulder at 300 nm which is the characteristic of PVP. All precursors did not show the spectrum in 400 nm. This illustrated that the precursors did not affect the plasmon band of silver nanoparticles.

Silver nanoparticles colloids with different concentrations (10 ppm, 7 ppm, 5 ppm, 3 ppm, and 1 ppm) had pale yellow color to dark pale yellow color as shown in Figure 4.9. From the study by UV-Visible spectroscopy, the plasmon extinction spectra of the synthesized PVP-stabilized silver nanoparticles have a plasmon extinction maximum (λ_{max}) at 403 nm and a shoulder at 350 nm and have a long tail in the longer wavelength region as shown in Figure 4.10. Taking into account the considerable scattering of these data we concluded that the sizes of silver nanoparticles with PVP are together formed small and very large sizes. Due to the observing that the plasmon maxima are shifted to the red and quadrupoles plasmon resonance is appeared in the spectra. According to Mie theory [23], the particles smaller than 20 nm show dipolar adsorption around 400 nm and the particles size under plasmon extinction spectra with quadrupole plasmon resonance are more than 40 nm. The FWHH is 70 nm. It indicates that the size distribution is broad corresponding to the different size of the synthesized silver nanoparticles.
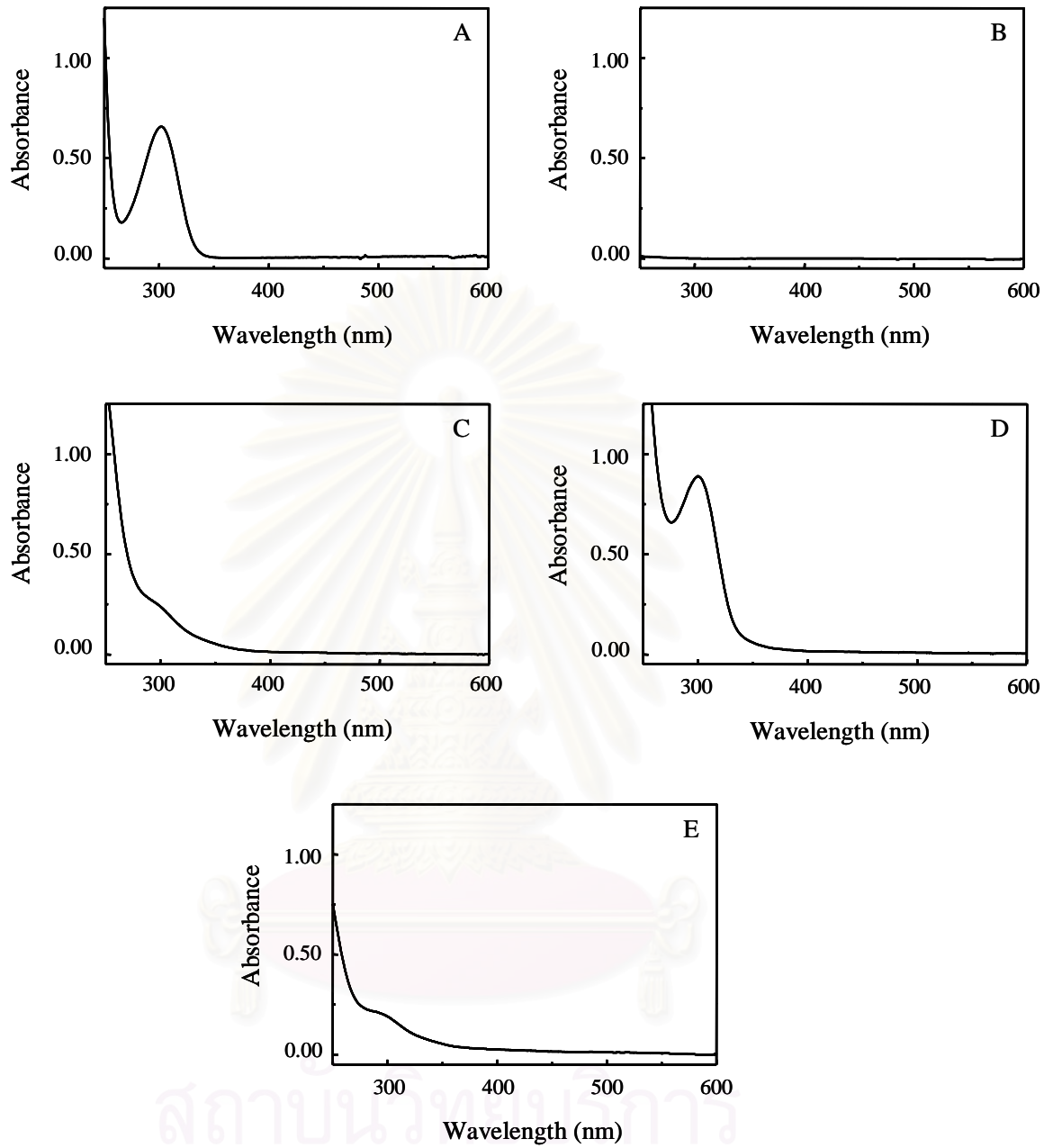
Figure 4.8   Absorption band of the precursors: the $AgNO_3$ solution (A), $NaBH_4$
             solution (B), 2 wt% PVP (C), $AgNO_3$ + 2 wt% PVP (D), and $NaBH_4$ +
             2 wt% PVP (E)

10 ppm   7 ppm   5 ppm   3 ppm   1 ppm
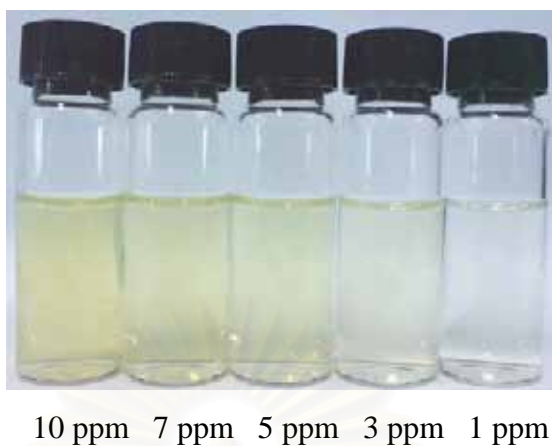
Figure 4.9   Appearance of various concentrations (10 ppm, 7 ppm, 5 ppm, 3 ppm, and 1 ppm) of silver nanoparticles with PVP as a stabilizer.
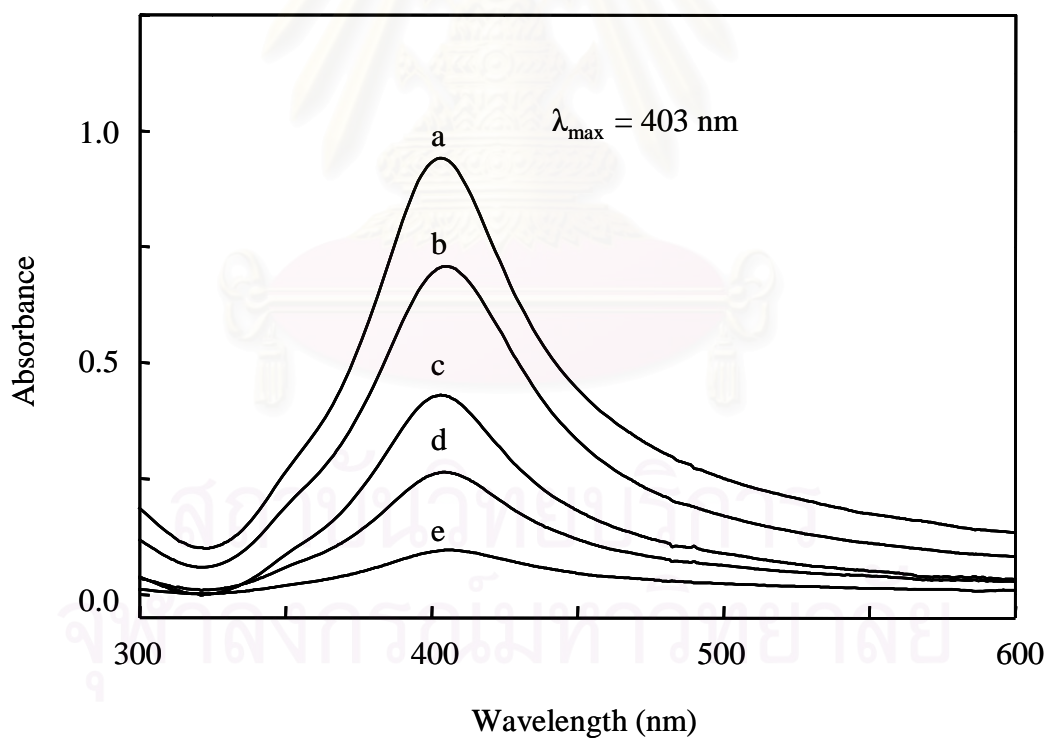
Figure 4.10   Plasmon extinction spectra of silver nanoparticles with PVP as a stabilizer: 10 ppm (a), 7 ppm (b), 5 ppm (c), 3 ppm (d), and 1 ppm (e).

4.2.2 Characterization of silver nanoparticles with PVP as a stabilizer by TEM

PVP-stabilized silver nanoparticles were characterized by TEM. Size, shape, and size distribution of PVP-stabilized silver nanoparticles are shown in Figure 4.11. It was shown that the shapes are rather spherical. The average size of silver nanoparticles with 200 particles is 18.27 nm. The particles sizes of PVP-stabilized nanoparticles are more than 45 nm which is consistent with the quadrupole plasmon resonance of spectra in Figure 4.10. Histogram of the size of silver nanoparticles is shown in Figure 4.11 (B) and the calculated standard deviation is about 10.43 nm. It indicates that size distribution is polydisperse. The mechanism can be explained as follows:

Mechanism of PVP-stabilized silver nanoparticles

The protection mechanism of PVP in the synthesis of silver nanoparticles is generally proposed on the basis of its structural features. PVP has a structure of a polyvinyl skeleton with polar group as shown in the Formula 1. The donated lone pairs electron of nitrogen and oxygen atoms in the polar groups of PVP may occupy two sp orbitals of silver ions to form a complex compound. According to literatures [46,47], the mechanism of PVP stabilized-silver nanoparticles can be explained as three steps. *The first step*, silver ions formed coordinative bonding with nitrogen and oxygen atoms of PVP as in Equation 2. *The next step*, PVP promotes the nucleation of silver nanoparticles because the Ag ions-PVP complex is more easily reduced than the pure Ag ions owing to Ag ions receiving more electronic clouds from PVP than from H_2O as in Equation 3. *Finally*, PVP protects the aggregation of silver nanoparticles by steric effect of long chain polyvinyl. These mechanisms are shown in Figure 4.12

A
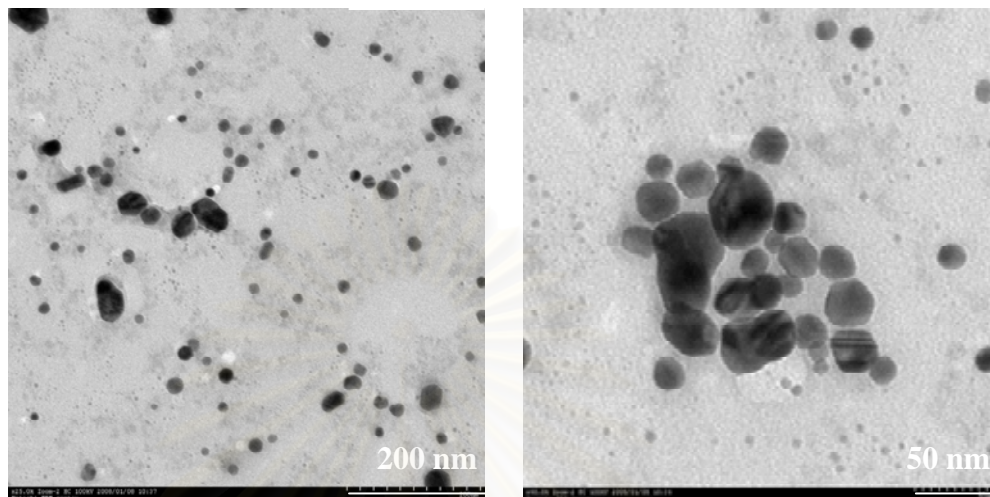
B
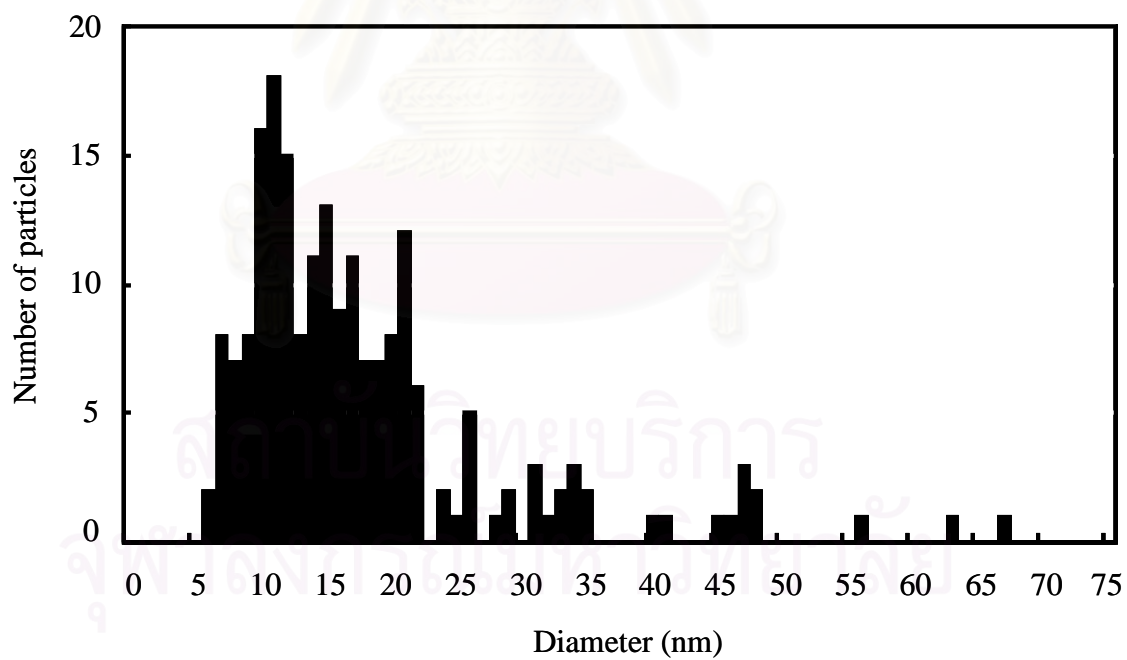
Figure 4.11   TEM images (A) and histogram (B) silver nanoparticles with PVP as a
                stabilizer.

——[CH$_2$——CH]$_n$——

[1]

[CH$_2$—CH] ... O + 2Ag$^+$ ⇌ [CH$_2$—CH] ...N:Ag$^+$: ... O + [CH$_2$—CH] ...N ... O: Ag$^+$:O ... N [CH$_2$—CH]

[2]

[CH$_2$—CH] [CH$_2$—CH] ...N:Ag$^+$: ... O + N ... O: Ag$^+$:O N [CH$_2$—CH] + 2e ⇌ [CH$_2$—CH] [CH$_2$—CH] ...N: Ag: ... O + N ... O: Ag :O N [CH$_2$—CH]

[3]

Figure 4.12   Schematic illustration of mechanism of the protection of PVP

4.2.3   Stability of silver nanoparticles with PVP as a stabilizer

The stability of PVP-stabilized silver nanoparticles remained after keeping for 3 months at room temperature. The plasmon extinction spectrum was investigated. Figure 4.13 displays the plasmon extinction spectra of silver nanoparticles with 1 day comparable with 3 months storage. After 3 months, the plasmon maximum spectrum shows at the same maximum wavelength but has a longer tail and the FWHH is about 75 nm. It showed that the particle sizes of silver nanoparticles with PVP increased.

Figure 4.13   Plasmon extinction spectra of silver nanoparticles with PVP as a stabilizer: 1day (a) and 3 months (b).

To confirm the particle sizes of silver nanoparticles after keeping for 3 months, it was characterized by TEM. The TEM images are shown in Figure 4.14 (A). It shows that the particle sizes is about 7-70 nm. The average size is 21.77 nm which calculated from 200 particles. Figure 4.14 shows the aggregation and growth of silver nanoparticles. The size distribution of silver nanoparticles was slightly broader than that of 1 day as shown in the histogram in Figure 4.14 (B) with standard deviation of 10.67 nm. This suggested that particles sizes had increased. From the result, it can be concluded that PVP was not a good stabilizer because the size of silver nanoparticles after 3 months increased. The efficiency of PVP is not enough to protect the aggregation of silver nanoparticles of high concentration.

A
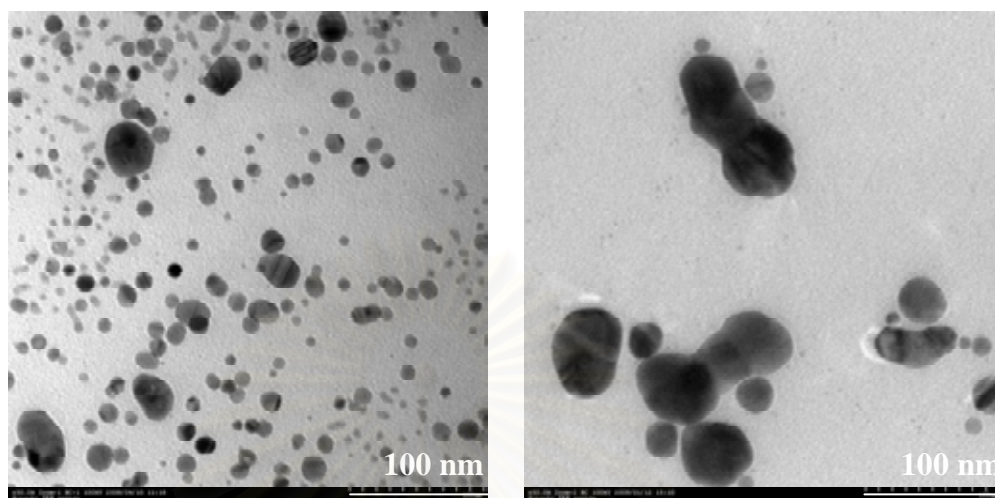
B
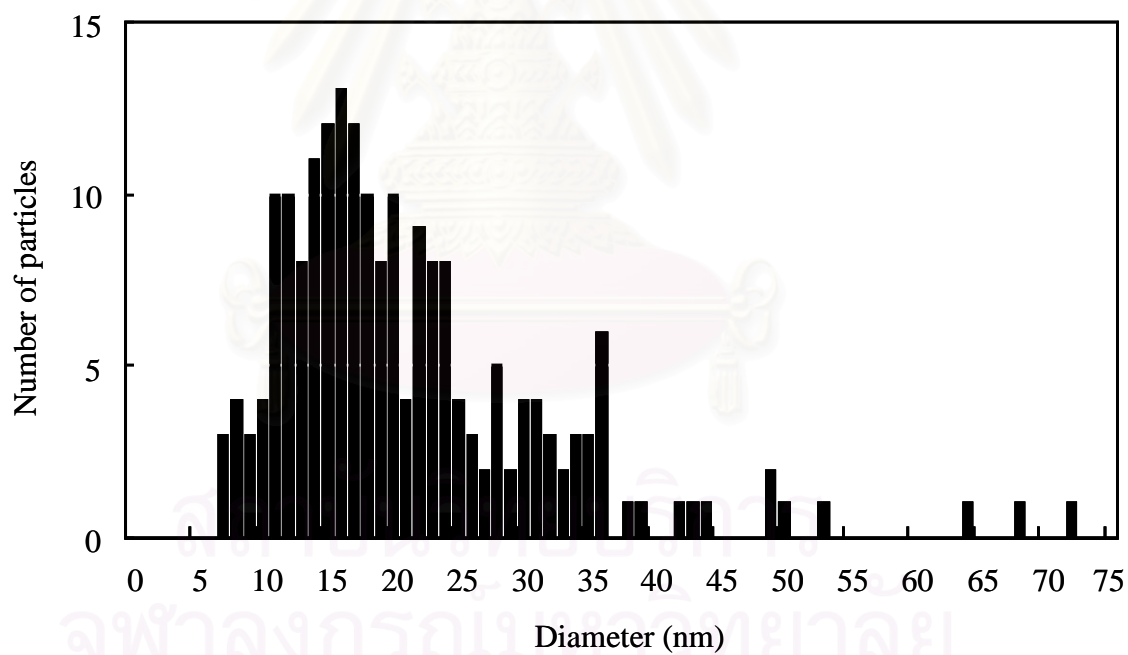
Figure 4.14   TEM images (A) and histogram (B) of silver nanoparticles with PVP
                as a stabilizer after keeping for 3 months at room temperature.

4.3   Synthesis of silver nanoparticles with starch as a stabilizer

In the synthesis of 10,000 ppm colloidal silver nanoparticles with starch as a stabilizer by reduction method, it was investigated that the color immediately changed when the first drop of $NaBH_4$ was added which showed the formation of silver nanoparticles. Finally, the solution has dark brown color which silver nanoparticles are formed as shown in Figure 4.15. When NaCl was added into the silver solution, no precipitation of AgCl occurred. It showed that silver ions completely converted to silver nanoparticles.

Figure 4.15   The synthesized silver nanoparticles with starch as a stabilizer: highly concentration (10,000 ppm) of silver nanoparticles.

4.3.1   Characterization of silver nanoparticles with starch as a stabilizer by Ocean Optics UV-Visible portable spectrometer

The precursors were characterized by Ocean Optics UV-Visible portable spectrometer before the synthesis of silver nanoparticles. Figure 4.16 shows the spectra of the precursors. Figure 4.16 (A and D) are the spectra of silver nitrate solution and silver nitrate solution with 2 wt% starch showing the absorption maxima at 300 nm of silver nitrate solution. Figure 4.16 (B) is the spectrum of sodium borohydride solution which does not appear in this region. Figure 4.16 (C and E) are the spectra of 2 wt% starch and sodium hydride with 2 wt% starch, respectively

showing the spectrum of 2 wt% starch. It indicated that the spectra of the precursors did not affect the plasmon band of starch-stabilized silver nanoparticles.

For characterization of 10,000 ppm of colloidal starch-stabilized silver nanoparticles by Ocean Optics UV-Visible portable spectrometer, the solution was diluted to 10 ppm, 7 ppm, 5 ppm, 3 ppm, and 1 ppm as shown in Figure 4.17. They are pale yellow to dark pale yellow, respectively.

The plasmon extinction spectra of silver nanoparticles with starch are shown in Figure 4.18 which plasmon bands are also symmetry and have plasmon extinction maximum at 397 nm. It should be noted that the particles shapes are spherical and sizes are very small due to the maxima at short wavelength of plasmon extinction spectrum, according to Mie theory [23]. And the plasmon bands are sharp and narrow FWHH are about 48 nm indicating that the size distribution is narrow.

4.3.2   Characterization of silver nanoparticles with starch as a stabilizer by TEM

The synthesized silver nanoparticles with starch were characterized by TEM. Figure 4.19 (A) is the TEM images showing size, size distribution and shape of starch-stabilized silver nanoparticles. It was found that the particles shapes were nearly spherical and size was about 5-20 nm. The average particles size was averaged from 200 particles, showing the average size was 11 nm. The size distribution of the synthesized silver nanoparticles is shown in histogram of Figure 4.19 (B). The standard deviation was 3.71 nm. This result shows that the particles size is almost monodisperse size distribution. It was confirmed that the result from TEM images were consistent with the plasmon extinction spectrum in Figure 4.18. It showed that starch was a good stabilizer to protect aggregation and aggromeration of silver nanoparticles.
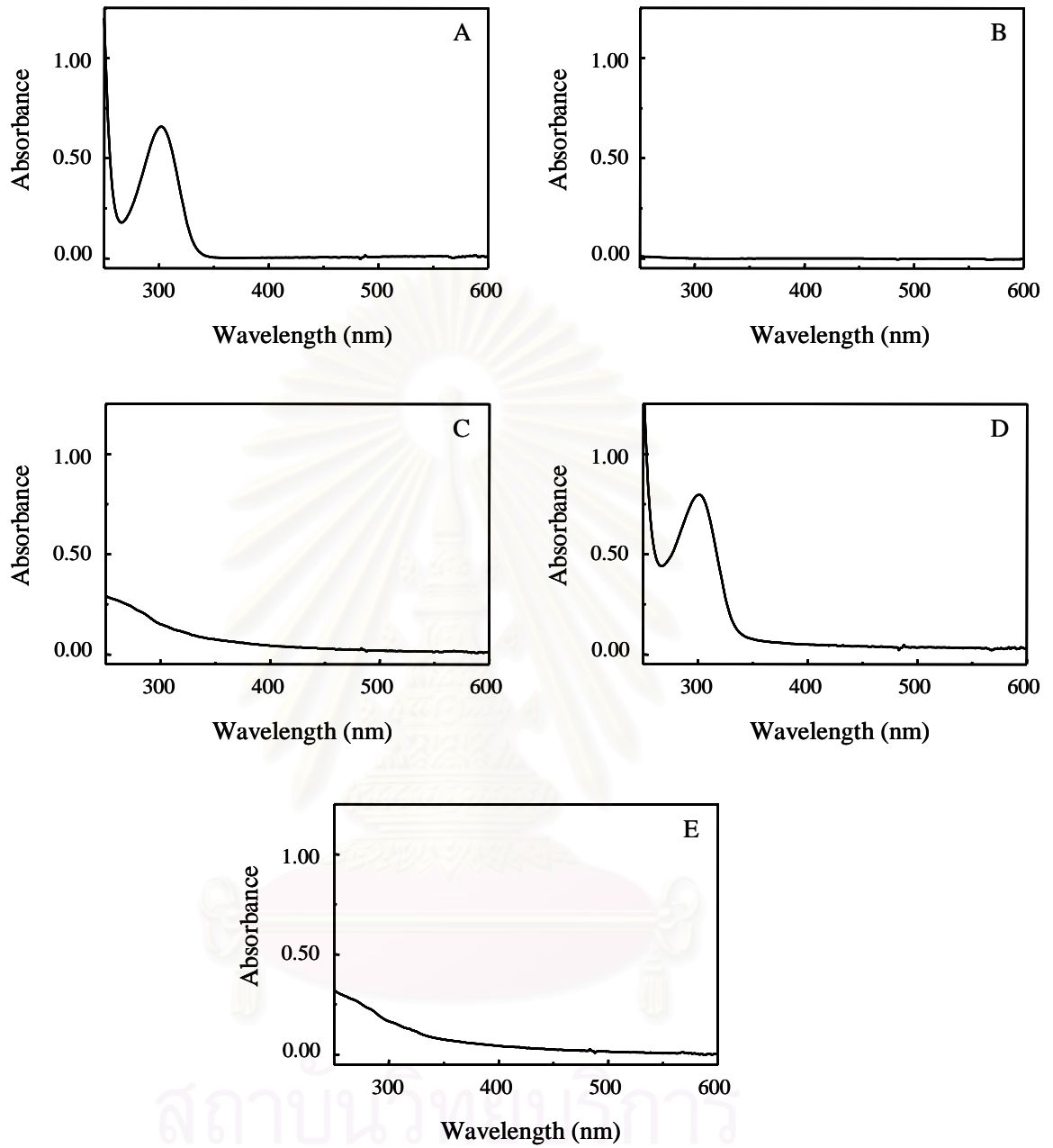
Figure 4.16   Absorption band of the precursors: the $AgNO_3$ solution (A), $NaBH_4$
              solution (B), 2 wt% starch (C), $AgNO_3$ + 2 wt% starch (D), and $NaBH_4$
              + 2 wt% starch (E).

10 ppm   7 ppm   5 ppm   3 ppm   1 ppm

Figure 4.17   Appearance of various concentrations (10 ppm, 7 ppm, 5 ppm, 3 ppm, and 1 ppm) of silver nanoparticles with starch as a stabilizer.
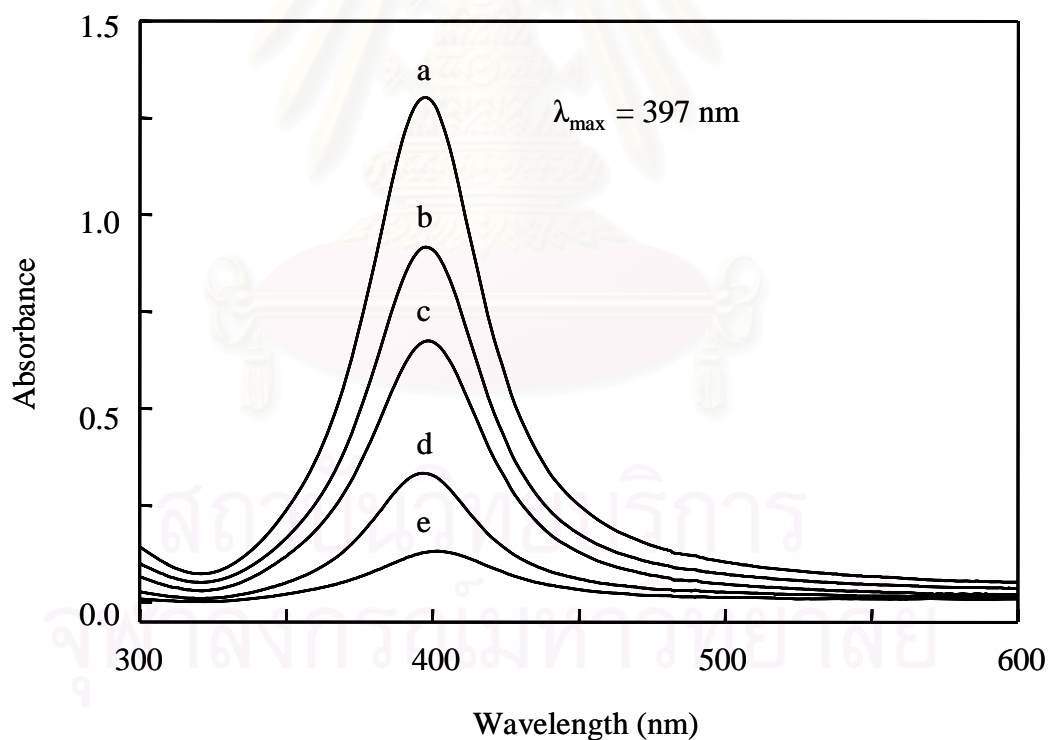
Figure 4.18   Plasmon extinction spectra of silver nanoparticles with starch as a stabilizer: 10 ppm (a), 7 ppm (b), 5 ppm (c), 3 ppm (d), and 1 ppm (e).
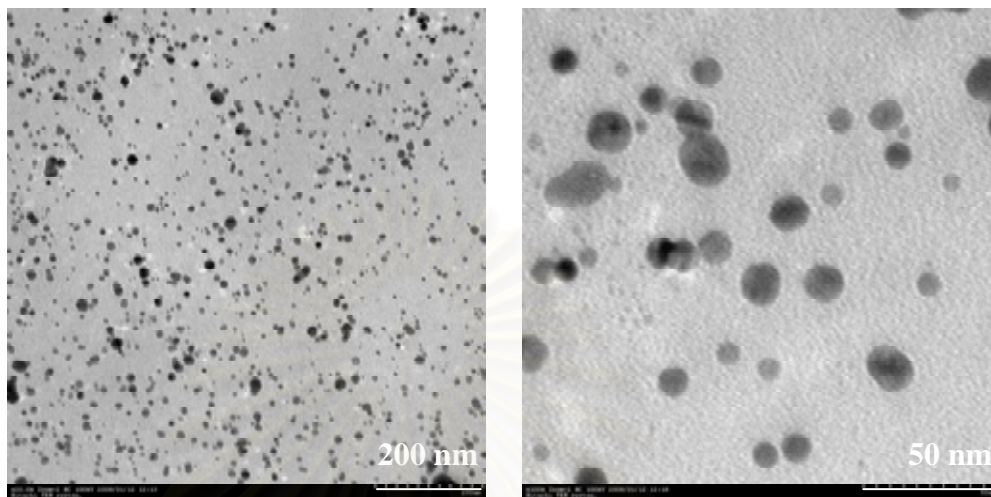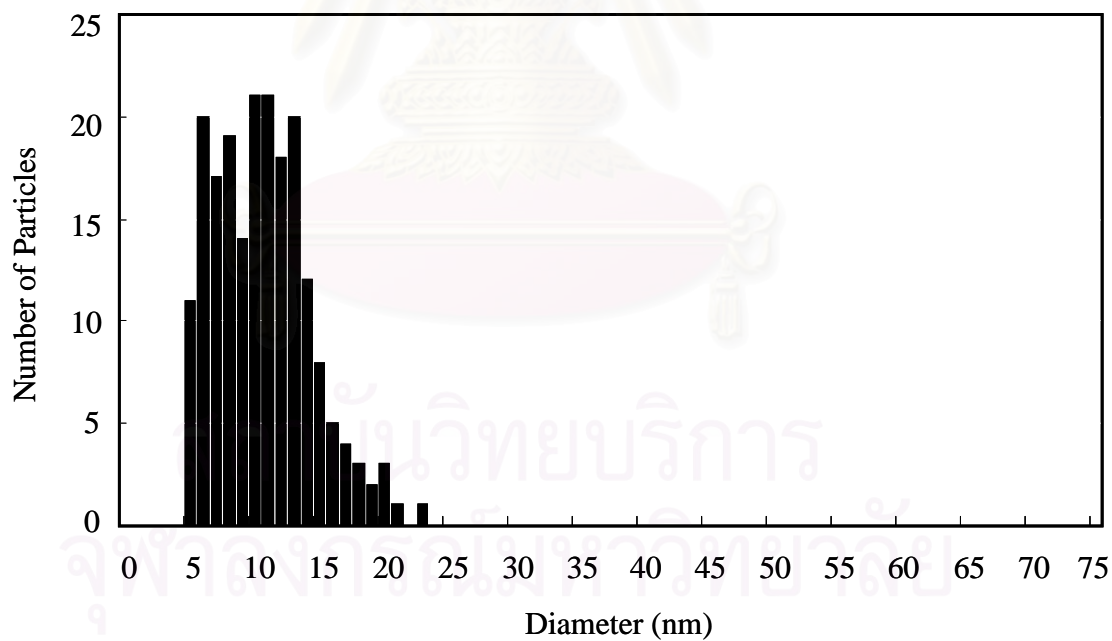
Figure 4.19   TEM images (A) and Histogram (B) of the silver nanoparticles with starch as a stabilizer.

Mechanism of starch-stabilized silver nanoparticles

The understanding of the mechanism of starch to stabilize silver nanoparticles has not yet known. In recent years, Vigneshwaran et. al. [48] synthesized silver nanoparticles with soluble starch as both the reducing agent as well as stabilizer. They revealed the number of hydroxyl groups in soluble starch complexed to silver ions and the aldehyde terminal reduced the silver ions. From iodometric titration confirmed that the silver nanoparticles were entrapped inside the helical amylose chains of the soluble starch. The synthesized silver nanoparticles size was about 10-34 nm.

Starch consists of amylose and amylopectin in ratio 20:80 or 30:70. Starch has a chemical formula as $(C_6H_{10}O_5)_n$. Both consist of polymers of α-D-glucose units in the $^4C_1$ conformation. Amylose are linked -(1 → 4)- glycosidic linkage with the ring oxygen atoms on the same side, whereas in amylopectin is linked -(1 → 6)- glycosidic linkage forming branch-pointed. In the synthesis, the starch from potato composes of amylose molecule. It is a linear polymer that the structure as shown in the Figure 4.20. When amylose is in aqueous solution at room temperature, it can form an extended shape and wind up into left-handed single helix or interrupted helix. If high molecular weight, amylose is formed left-handed double helix. Single helical amylose has hydrogen bonding between O2 and O6 atoms on the outside surface of the helix with only the ring oxygen pointing inwards. These helical are stiff. The single helix, interrupted helix and double helix as shown in Figure 4.21 [49].
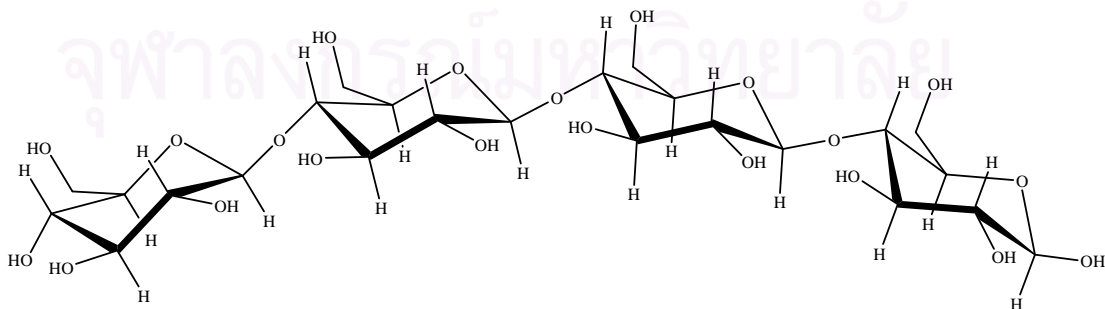
Figure 4.20   Structure of amylose with -(1 → 4)- glycosidic linkage.

A: single helix   B: Interrupted helix   C: Double helix
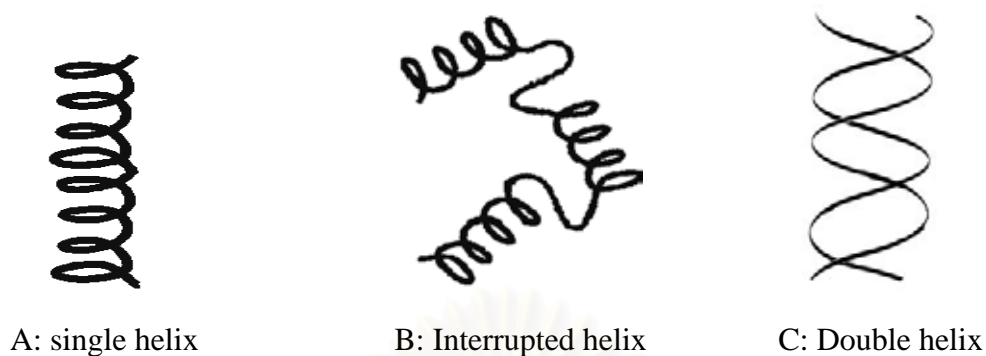
Figure 4.21   Helix of amylose in aqueous solution.

Silver nanoparticles can be stabilized by entrapping inside the helical amylose chain, according to the literature reviews [48]. Furthermore, silver ions can form coordination bond with oxygen atoms of hydroxyl groups in amylose. Additionally speaking, the steric of starch molecule in helix formed protects the aggregation of silver nanoparticles.

4.3.3   Stability of silver nanoparticles with starch as a stabilizer

The stability of starch-stabilized silver nanoparticles was monitored for 3 months at room temperature. Plasmon extinction spectrum of silver nanoparticles with starch as a stabilizer is shown in Figure 4.22. The spectrum is sharp and shows plasmon extinction maximum at 400 nm which shifts from the origin spectrum about 3 nm. It indicated that the size of silver nanoparticles increased slightly. The FWHH is 51 nm which is somewhat broader than that of the nearly synthesized particles. This result shows that the size distribution of silver nanoparticles is increased.

It was confirmed by TEM images as shown in Figure 4.23 that the starch stabilized silver nanoparticles show little growth with a average particles size of 14.90 nm. No changing was registered on the shape of the particles as shown in Figure 4.23 (A). The size distribution of the starch-stabilized silver nanoparticles is shown in Figure 4.23 (B). The standard deviation was 4.42 nm. It indicated that the size distribution of silver nanoparticles after keeping for 3 months at room temperature is slightly broader than that of the nearly synthesized particles. Silver nanoparticles with starch are stable with a little change of their appearance or a property, showing that starch was a good stabilizer for the colloidal silver nanoparticles.

Figure 4.22   Plasmon extinction spectra of silver nanoparticles with starch as a stabilizer: 1 day (a) and 3 months (b).

(A)

(B)

Figure 4.23   TEM images (A) and histogram (B) of silver nanoparticles with starch
              as a stabilizer after keeping for 3 months at room temperature.
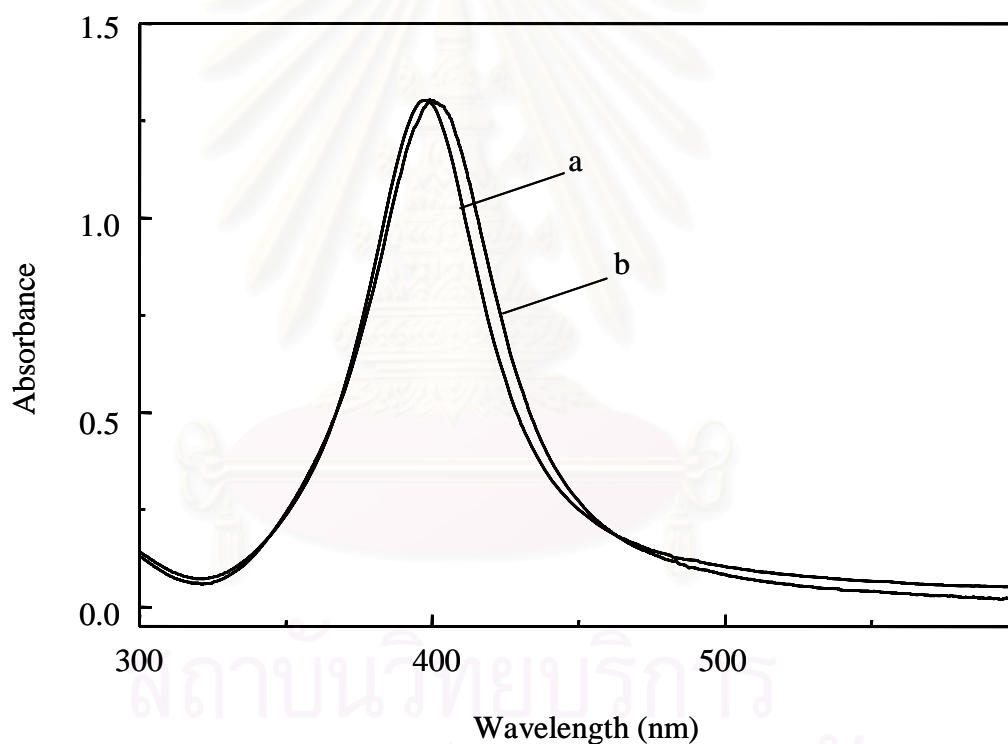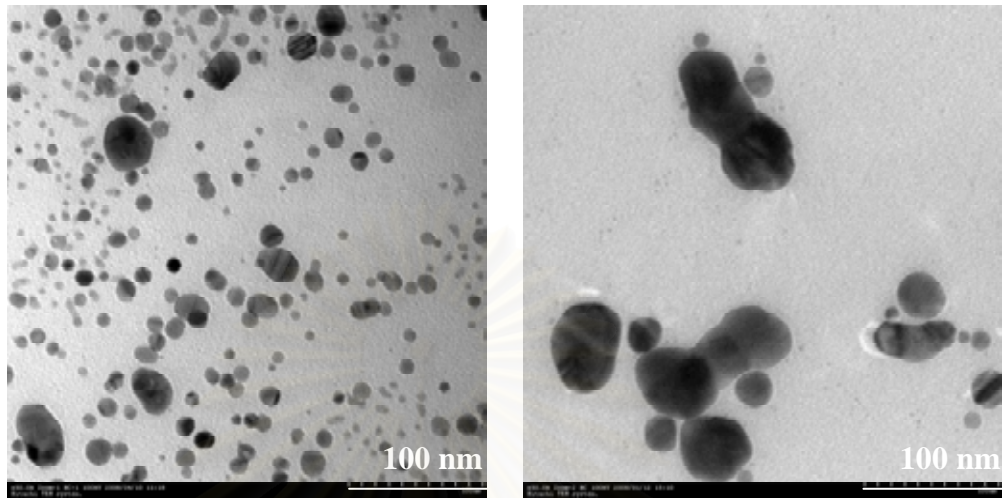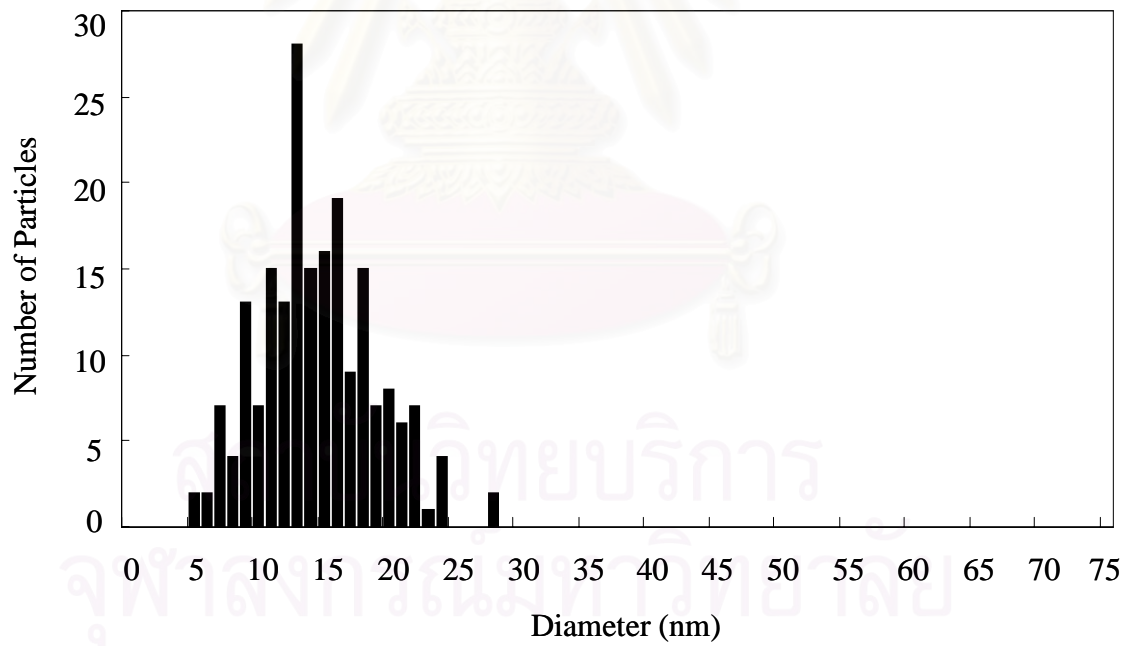
4.4   Comparison of silver nanoparticles with various stabilizers

The plasmon extinction spectra of gelatin, PVP, and starch-stabilized silver nanoparticles are shown in Figure 4.24. When starch was used as a stabilizer, plasmon extinction maximum (λ_{max}) and FWHH are 397 nm and 48 nm, respectively which are sharper and narrower than that of gelatin and PVP as the stabilizers. Due to plasmon maximum of PVP and gelatin-stabilized silver nanoparticles are 403 nm and 410 nm. FWHH of PVP and gelatin-stabilized silver nanoparticles are 70 nm and 75 nm. This indicated that sizes and size distribution of silver nanoparticles with starch are smaller and more uniform than the nanoparticles with gelatin and PVP. The spectrum of PVP-stabilized silver nanoparticles shows *quadrupole plasmon resonance* at 350 nm while the spectrum of gelatin-stabilized silver nanoparticles did not occur. It indicates that the formations of PVP-stabilized silver nanoparticles are together small and very large which more than 40 nm. In addition, FWHH of gelatin-stabilized silver nanoparticles are narrower than that of PVP-stabilized silver nanoparticles. This indicates that size distribution of gelatin-stabilized silver nanoparticles are narrower than that of PVP-stabilized silver nanoparticles. At the same concentration, the absorbance of starch-stabilized silver nanoparticles is higher than that of PVP and gelatin. It means that amount of particles with starch are higher than the others.

Additionally, transmission electron microscopy has further been applied to validate the existence of small nanoparticles which confirms that the average size of starch-stabilized silver nanoparticles are about 11 nm, much smaller than that of silver nanoparticles with gelatin and PVP as the stabilizers. The average particles sizes of silver nanoparticles of gelatin and PVP-stabilized silver nanoparticles are 19.54 and 18.27 nm, respectively as shown in Figure 4.25. Furthermore, to monitor the stability of the final synthesized silver nanoparticles, the plasmon extinction spectra were measured for 3 months and size and size distribution were characterized.
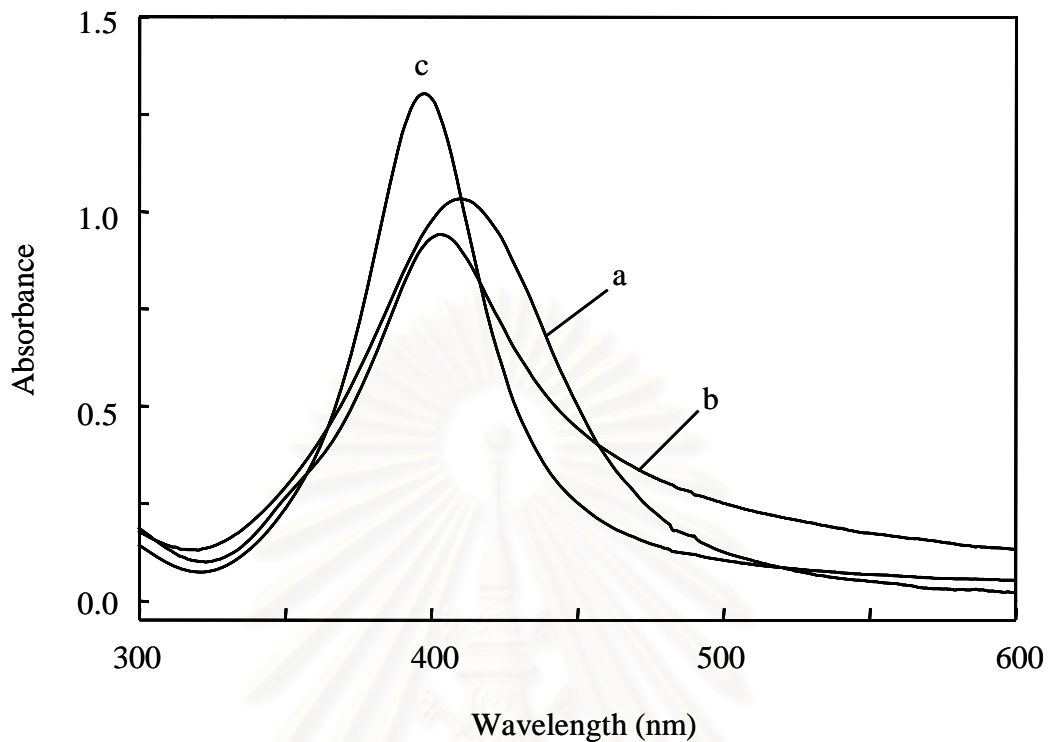
Figure 4.24   Plasmon extinction spectra of silver nanoparticles with gelatin (a), starch (b), and PVP (c) as a stabilizer.
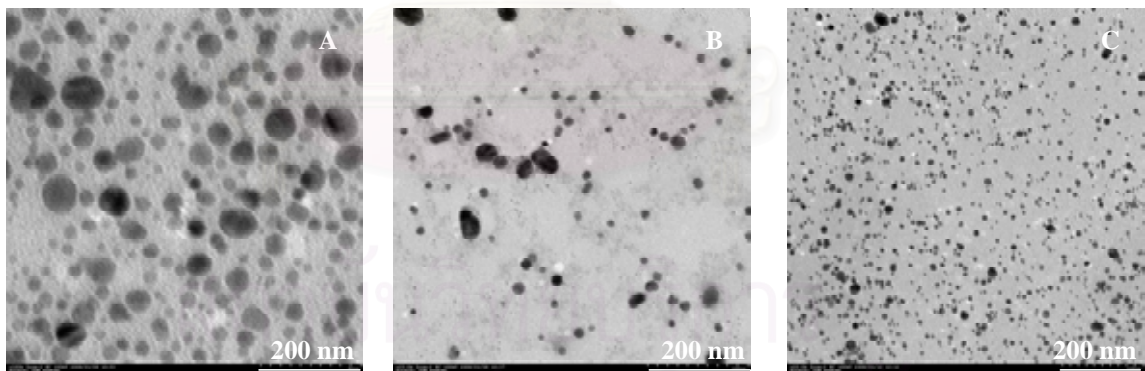
Figure 4.25   TEM images of silver nanoparticles with various stabilizers: (A) gelatin-stabilized silver nanoparticles, (B) PVP-stabilized silver nanoparticles, and (C) starch-stabilized silver nanoparticles.

In order to compare the characteristics of silver nanoparticles with various stabilizers are summarized in Table 4.2 and Table 4.3. From Table 4.2, it shows the characteristic of silver nanoparticles with various stabilizers. Table 4.3 shows the characteristic of silver nanoparticles with various stabilizers after keeping for 3

months. It showed that the stability of silver nanoparticles with starch and PVP remained for at least 3 months but size and size distribution of silver nanoparticles with starch were smaller than that of silver nanoparticles with PVP. Gelatin-stabilized silver nanoparticles precipitated after 5 days. The stability of silver nanoparticles was highest in starch followed by PVP, and in gelatin it was the least stable. Thus, starch was identified as the best stabilizer for the synthesized silver nanoparticles became observing that after 3 months the particles sizes and shape did not change. Since the structure of starch is helix and steric hindrance of starch molecule formed around the particles to preventing them from aggregation greatly by electrostatic interactions.

Table 4.2   Characteristics of silver nanoparticles with various stabilizers.

Stabilizer	Plasmon extinction maximum, λ_{max} (nm)	Full Width at Half Height, FWHH (nm)	Average particles size from TEM (nm)	Stability
gelatin	410	75	19.54	~ 5 days*
PVP	403	70	18.27	> 90 days
starch	397	48	11	> 90 days

* precipitate occur after 5 day

Table 4.3   Characteristics of silver nanoparticles with various stabilizers after 3 months.

Stabilizer	Plasmon extinction maximum, λ_{max} (nm)	Full Width at Half Height, FWHH (nm)	Average particles size from TEM (nm)
gelatin	precipitation	precipitation	precipitation
PVP	403	75	14.90
starch	400	51	21.77

4.5   Characterization of silver-coated cotton and polyester fabrics

Silver nanoparticles with smallest size and having a very narrow size distribution and highly stabilization is used in the padding process for immobilization them on cotton and polyester fabrics. Silver nanoparticles with starch as a stabilizer were used in this process.

The size of cotton and polyester fabrics size were 10×15 cm^2. These fabrics were padded through starch-stabilized silver nanoparticles solution bath. Concentrations of silver nanoparticles used in this study were 12.5 ppm, 25 ppm, 62.5 ppm, 125 ppm, and 250 ppm. The pressure of padder was 3.0 bars. The wet pick-up ratio of cotton and polyester was 80%. The real concentrations of silver nanoparticles on the fabrics were 10 ppm, 20 ppm, 50 ppm, 100 ppm, and 200 ppm. The fabrics were run through the padder that forced the silver nanoparticles solution into the fabrics with pressure.

The cottons and polyester fabrics without silver nanoparticles and the cottons and polyester fabrics after coating silver nanoparticles are shown in Figure 4.26. The original colors of the fabrics (cottons and polyesters) are white. After passing through the bath of silver solution, padder, and dry in oven, colors of the both fabrics change into yellow color due to the yellow color of silver nanoparticles. At higher concentrations, the colors of the fabrics are darker than that of lower concentrations. It showed that silver nanoparticles were immobilized on the fabrics. The immobilizations on fabrics depend on the concentration of silver nanoparticles in the bath.

Due to the structure of cotton fabrics having hydroxyl group as shown in the Figure 4.27, the chemical reactivity of cotton is related to the hydroxyl group (-OH) of the glucose unit [50]. The hydroxyl group binds readily with silver nanoparticles in water base.
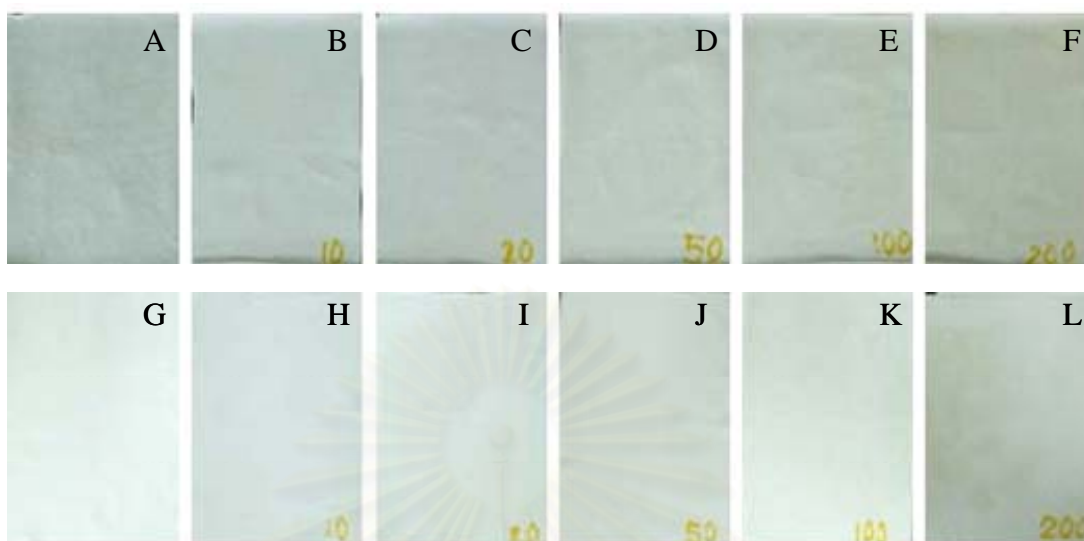
Figure 4.26   The silver-coated cotton and polyester fabrics with various concentration after passing through padding process: blank cotton fabrics (A), blank polyester fabrics (G), 10 ppm (B), (H), 20 ppm (C), (I), 50 ppm (D), (J), 100 ppm (E), (K), 200 ppm (F), (L) of silver nanoparticles on cotton and polyester fabrics, respectively.
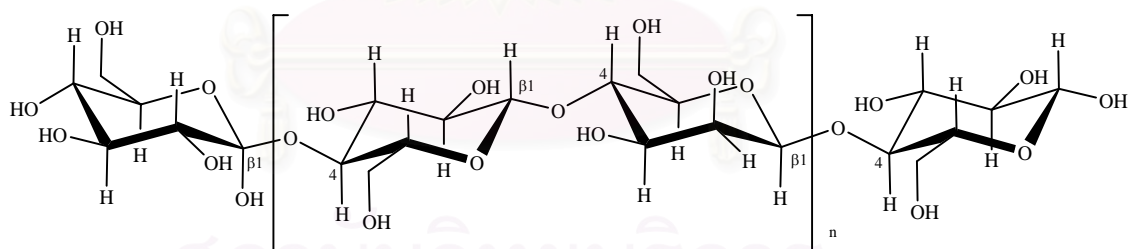
Figure 4.27   Molecular structure of cotton fibers.

In the case of polyester fabrics, polyester is produced by reacting dicarboxylic acid with dihydric alcohol which contains the ester groups in their main chain at least 85% by weight of the total polymer content as follows:
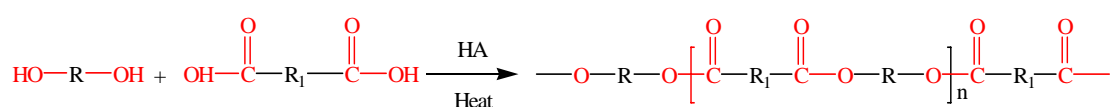
The molecular chains of polyester fibers are packed closely together and are well oriented. Polyester fibers are smooth fibers with a circular cross section [50]. The ester groups of polyester fabrics react with silver nanoparticles in water base.

In addition, starch as a stabilizer consists of α-D-glucose units which have hydroxyl groups in the structure. The hydroxyl group of glucose of starch can be formed hydrogen bonding with hydroxyl group of glucose of cotton or ester groups of polyester fabrics. Silver nanoparticles with starch as a stabilizer are well absorbed on the cotton and polyester fabrics.

When comparing cotton with polyester fabrics, it shows that the color of cotton is yellow but it is darker than the color of polyester fabrics. This indicates that the amount of silver nanoparticles on cotton are more than that of polyester fabrics possibly due to the close packing and smooth surface contour of polyester fibers. The surface area of polyester fibers is low when comparing with cotton fibers. The surface contours of cotton fibers are rough and striated and shape are ribbonlike twists. The surface area of cotton fibers is high. The cross section and surface contour of cotton and polyester fibers are shown in Figure 4.28 [50]. Therefore, these results conclude that cotton is more absorbable silver nanoparticles solution than polyester fabric as a resulting in the cotton of color has a yellow darker than the polyester of color.

A: B:
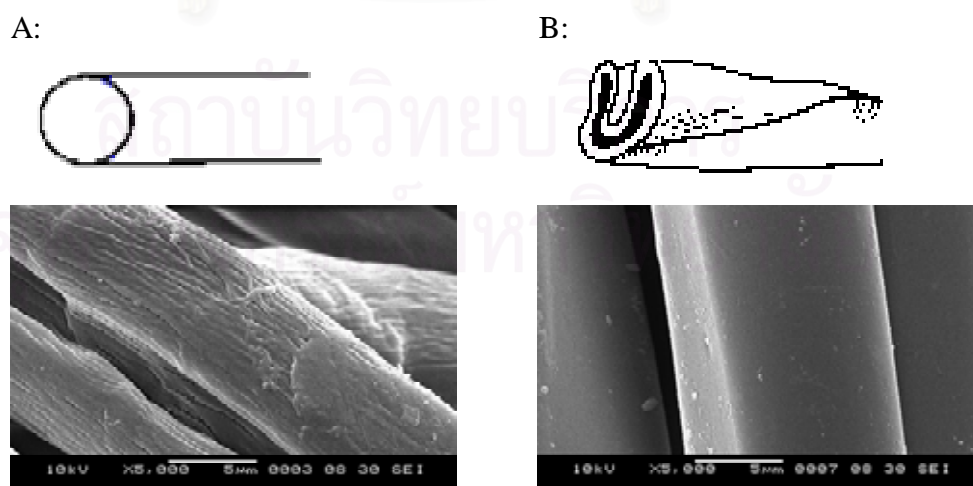
Figure 4.28   Cross-section and shape contour of cotton (A) and polyester (B) fibers [50].

4.5.1 Characterization of silver nanoparticles on cotton and polyester fabrics by SEM

Cotton and polyester fabrics were padded through silver solution bath. Silver nanoparticles were immobilized on these fabrics. Cotton and polyester fabrics with silver nanoparticles of 10 ppm, 20 ppm, 50 ppm, 100 ppm, and 200 ppm were characterized by SEM. Blank cotton and blank polyester were also characterized as a reference. These fabrics are shown in Figure 4.29. The amounts of silver nanoparticles on cotton and polyester fabrics correspond to the concentration of silver nanoparticles solution. At the same concentration, the amounts of silver nanoparticles on the cotton fabrics are more than that on the polyester fabrics, consistent with the color of these fabrics in Figure 4.28. The blank cotton and polyester fabrics are shown in Figure 4.29 (A and B). These show that the surfaces of cotton fibers are rough and striated and that of polyester fibers are smooth. These results confirm that the immobilizations of silver nanoparticles on cotton fabrics are more than that of polyester fabrics.

From SEM images, they show that silver nanoparticles were well-dispersed on the fabrics surface. The padding method is a suitable process for application of textile industry because it is simple and does not change the process or the machine of factory.
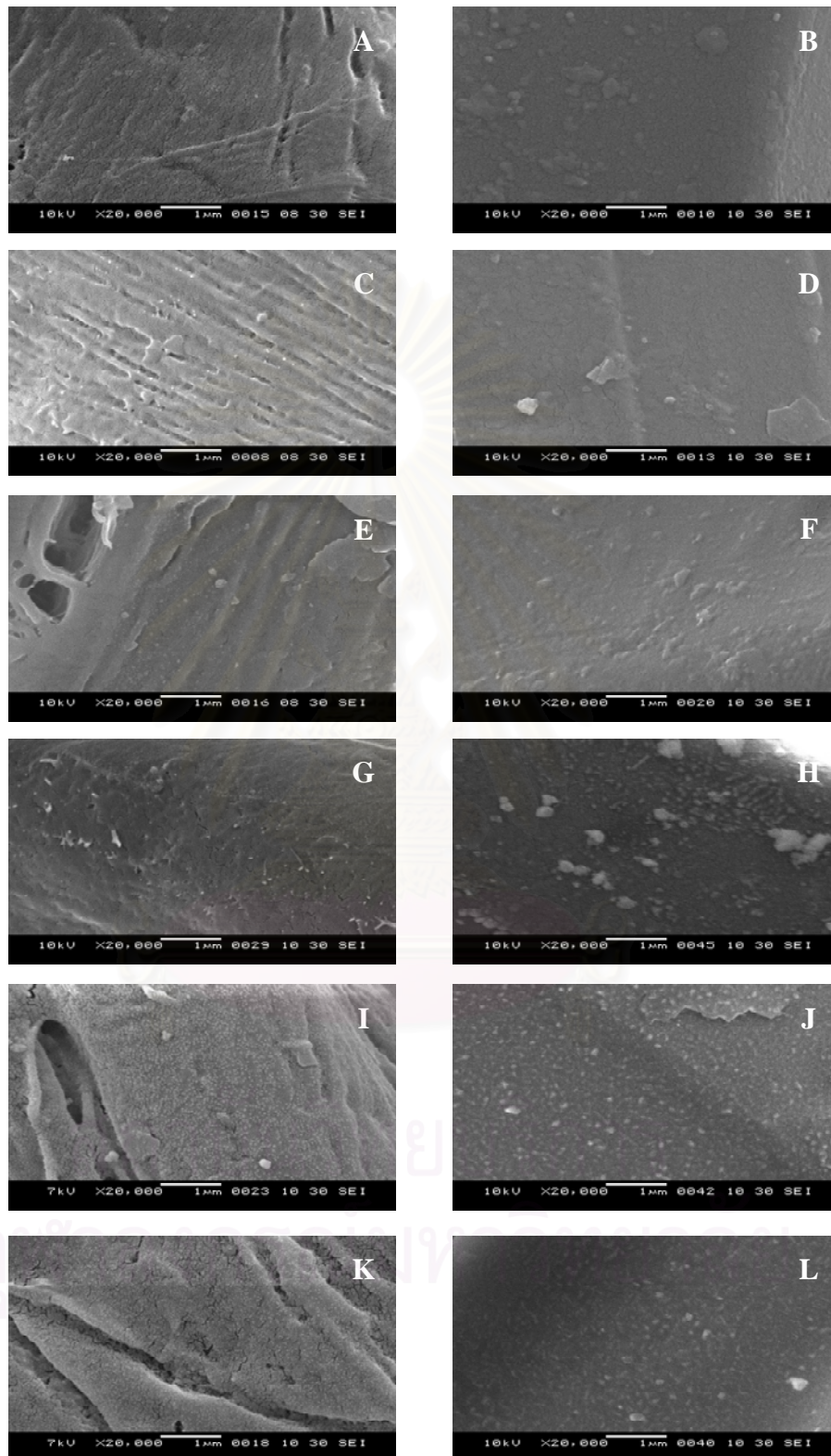
Figure 4.29   SEM images of silver-coated cotton (left row) and polyester (right row): blank (A), (B), 10 ppm (C), (D), 20 ppm (E), (F), 50 ppm (G), (H), 100 ppm (I), (J) and 200 ppm (K), (L) of silver nanoparticles.

4.6 Antibacterial test of silver nanoparticles on cotton and polyester fabrics

The antibacterial activity of silver-coated cotton and polyester fabrics were investigated against *S. aureus* by AATCC test method 147-1998 of the American Association of Textiles Chemist and Colorists. The 20 and 50 ppm silver nanoparticles on the fabrics were tested. The 20 and 50 ppm silver-coated fabrics washed were 20 times before antibacterial test. The washed 50 ppm silver-coated fabrics were characterized by SEM. The SEM images of the washed fabrics are shown in Figure 4.30. From SEM images, silver nanoparticles were well immobilized on the fabrics after 20 washing times. It shows that the padding method is suitable for the immobilization of silver nanoparticles on the fabrics.
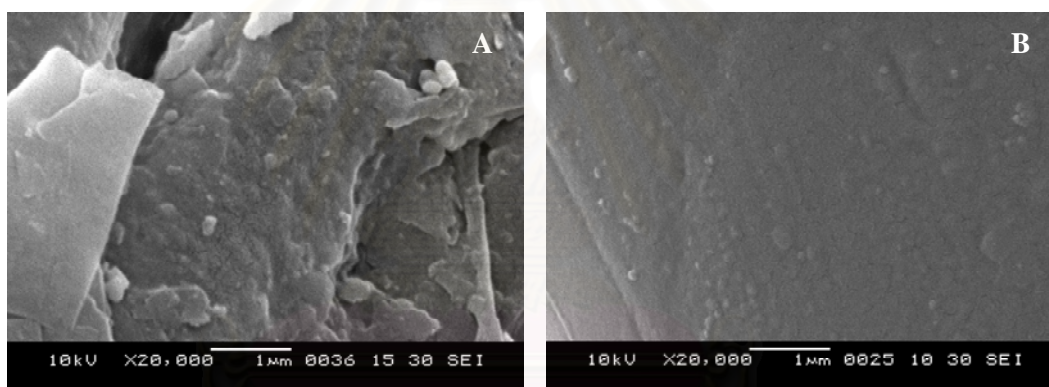
Figure 4.30   SEM images of 50 ppm silver nanoparticles on the fabrics after 20 times washing fabrics: cotton (A) and polyester (B) fabrics.

The silver-coated cotton and polyester fabrics after 20 washes were tested. These fabrics samples were placed directly on the top of the streaks in nutrient. The dishes were then incubated for 24 hours at 37°C. The results of the antibacterial tested are shown in Table 4.4. In the contact with blank cotton and blank polyester, there were light bacterial growth and moderated bacterial growth, respectively. They show that no inhibition of bacterial growth in contact area. In contact with silver-coated fabrics, the plates were examined for the inhibition of growth underneath and near the

edge of the test fabrics along each streak of inoculums. No bacterial growth occurred in contact area. They showed inhibited bacterial growth.

As mentioned before [51], bicomponent sheath-core fibers were prepared by a general melt-spinning method with polypropylene chips and silver nanoparticles. The fiber with silver nanoparticles in core part did not show antibacterial effects, while fiber with silver nanoparticles in sheath part exhibited excellent antibacterial effects. It showed that silver nanoparticles on the surface fabrics exhibit the highest antibacterial efficacy. This result confirmed the immobilizations of the silver nanoparticles on fabrics were carried out by padding process. Silver nanoparticles on the fabric can still show the antibacterial properties.

Table 4.4   The antibacterial properties of 20-wash silver nanoparticles-coated cotton and polyester fabrics.

S. aureus	Bacteria Growth		
Sample	Blank	20 ppm AgNPs	50 ppm AgNPs
cotton	LG	NG	NG
polyester	MG	NG	NG

Where NG   -   No growth under the sample in the contact area

LG   -   Light growth under the sample in the contact area

MG   -   Moderate growth under the sample in the contact area

CHAPTER V

CONCLUSIONS

Stable and highly concentrated (10,000 ppm) colloidal silver nanoparticles were synthesized by the chemical reduction method in the presence of stabilizers. The silver salts and reducing agent were silver nitrate and sodium borohydride, respectively. In this study, biocompatible materials as well as gelatin, PVP, and starch were used as a stabilizer in order to study the efficiency of these stabilizers for preventing the aggregation of the synthesized silver nanoparticles. When starch was used as the stabilizer, the silver nanoparticles were the smallest as well as the most narrow size distribution. The plasmon extinction spectrum of starch-stabilized silver nanoparticles shows the absorption maxima at 397 nm and FWHH at 48 nm while these of gelatin and PVP-stabilized silver nanoparticles show the absorption maxima at 410 and 403 nm and FWHH at 75 and 70 nm, respectively. The result from TEM confirms that the size of silver nanoparticles with starch as a stabilizer is about 5-20 nm on the average size of 11 nm. While gelatin and PVP as a stabilizer, the average sizes are 19.54 and 18.27 nm, respectively. From these results, it indicates that starch-stabilized silver nanoparticles have the smallest size and narrow size distribution.

Silver nanoparticles with starch as a stabilizer are used to immobilize on the cotton and polyester fabrics by padding process. The TEM images show well dispersion of silver nanoparticles on the fabrics. Silver nanoparticles are adsorbed on the cotton fabrics more than that on the polyester fabrics due to the molecular structure of cotton fabrics.

The antibacterial property of silver nanoparticles at concentration of 20 and 50 ppm on cotton and polyester fabrics after 20 washes are studied to confirm the immobilization of silver nanoparticles on the fabrics. The washed fabrics show

excellent antibacterial effect. Immobilization of silver nanoparticles on cotton and polyester were carried out by padding process.

REFERENCES

[1] Sonnichsen, C. Plasmons in metal nanostructures. Dissertation, Physics Department, Ludwig-Maximilians-University of Munich, 2001.

[2] White J. M. L.; Powell, A. M.; Bradyt, K.; and Russell-Jones, R. Severe generalized argyria secondary to ingestion of colloid silver protein. Clin. Exp. Dermatol. 28 (2002): 254-256.

[3] Sondi, I.; and Salopek-Sondi. B. Silver nanoparticles as antimicrobial agent: A case study on *E. coli* as a model for gram-negative bacteria. J. Colloid. Interf. Sci. 275 (2004): 177-182.

[4] Yu, D. G.; Lin, W. C.; Lin, C. H.; Chang, L. M.; and Yang, M. C. An in situ reduction method for preparing silver/poly(vinyl alcohol) nanocomposites as surface-enhanced Raman scattering (SERS)-active substrates. Mater. Chem. Phys. 101 (2007): 93-98.

[5] Zhou Z.; et al. Novel synthesis of highly active Pt/C cathode electrocatalyst for direct methanol fuel cell. Chem. Commun. (2003): 394-395.

[6] Cheng, D.; Yang, J.; and Zhao, Y. Antibacterial materials of silver nanoparticles application in medical appliances and appliances for daily use. Chin. Med. Equip. J. 4 (2004) 26-32.

[7] Dawn, A.; Mukherjee, P.; and Nandi, A. K. Preparation of size-controlled, highly populated, stable, and nearly monodispersed Ag nanoparticles in organic medium from a simple interfacial redox process using a conducting polymer. Langmuir 23 (2007) 5231-5237.

[8] Xie, Y.; Ye, R.; and Liu. H. Synthesis of silver nanoparticles in reverse micelles stabilized by natural biosurfactant. Colloids. Surf. *A* 279 (2006): 175-178.

[9] Liu, F. K.; Ko, F. H.; Huang, P. W.; Wu, C. H.; and Chu, T. C. Studying the size/shape separation and optical properties of silver nanoparticles by capillary electrophoresis. J. Chromatogr. A 1062 (2005) 139-145.

[10] Kometani, N.; Kohara, Y.; and Yonezawa, Y. Preparation of colloidal silver nanoparticles using benzoin as a photoinitiator. Colloids. Surf. A 313-314 (2008) 43-46.

[11] Lee, G. J.; Shin, S. I.; Kim, Y. C.; and Oh, S. G. Preparation of silver nanorods through the control of temperature and pH of reaction medium. Mater.Chem. Phys. 84 (2004): 197-204.

[12] Yu, Y. Y.; Chang, S. S.; Lee, C. L.; and Wang, C. R. C. Gold nanorods: electrochemical synthesis and optical properties. J. Phys. Chem. B 101 (1997): 6661-6664.

[13] Jana N. R.; Gearheart, L.; and Murphy, C. J. Wet Chemical Synthesis of High Aspect Ratio Cylindrical Gold Nanorods. J. Phys. Chem. B 105 (2001): 4065-4067.

[14] Henglein, A. Colloidal silver nanoparticles: photochemical preparation and interaction with O_2, CCl_4, and some metal ions. Chem. Mater. 10 (1998): 444-450.

[15] Park, K.; Seo, D.; and Lee, J. Conductivity of silver paste prepared from nanoparticles. Colloids. Surf. A 313-314 (2008): 351-354.

[16] Sondi, I.; and Salopek-Sondi, B. Silver nanoparticles as antimicrobial agent: a case study on E. coli as a model for Gram-negative bacteria. J. Colloid Interface Sci. 275 (2004): 177-182.

[17] Pal, S.; Tak, Y. K.; and Song, J. M. Does the Antibacterial Activity of Silver Nanoparticles Depend on the Shape of the Nanoparticle? A Study of the Gram-Negative Bacterium Escherichia coli. Appl. Environ. Microbiol. 73 (2007): 1712-1720.

[18] Ales, P. et al. Silver colloid nanoparticles: synthesis, characterization, and their antibacterial activity. J. Phys. Chem. B 110 (2006): 16248-16253.

[19] Sondi, I.; Goia, D. V.; and Matijevic, E. Preparation of highly concentrated stable dispersions of uniform silver nanoparticles. J. Colloid. Interf. Sci. 260 (2003): 75-81.

[20] Lee, C. L.; and Wan, C. C. Process for Preparing noble metal nanoparticles. US Patent 6,572,673 B2 (2003).

[21] Liu, J.; Lee, J. B.; Kim, D. H.; and Kim, Y. Preparation of highly concentration of silver colloidal nanoparticles in layered laponite sol. Colloids. Surf. A 302 (2007): 276-279.

[22] Maier S. A. Plasmonics: fundamentals and applications The United State of America: Springer Science + Busniness Media LLC., 2007

[23] Noguez, C. Surface plasmons on metal nanoparticles: The influence of shape and physical environment. J. Phys. Chem. C 111 (2007): 3806-3319.

[24] Malinsky, M. D.; Kelly, K. L.; Schatz G. C.; and Van Dunye, R. P. Nanosphere lithography: Effect of substrate on the localized surface plasmon resonance spectrum of silver nanoparticles. J. Phys. Chem. B 105 (2001): 2343-2350.

[25] Willets, K. A.; and Van Duyne, R. P. Localized surface plasmon resonance spectroscopy and sensing. Annu. Rev. Phys. Chem. 58 (2007): 67-97.

[26] Haes, A. J.; and Van Duyne, R. P. A unified view of propagating and localized surface plasmon resonance biosensors. Anal. Bioanal. Chem. 379 (2004): 920-930.

[27] Sergeev G. B. Nanochemistry. Laboratory of low temperature chemistry, Moscow: Elsevier, 2006.

[28] Shirtcliffe, N.; Nickel, U.; and Schneider, S. Reproducible preparation of silver sols with small particle size using borohydride reduction: for use as nuclei for preparation of larger particles. J. colloid Interface Sci. 211 (199): 122-129.

[29] Kadolph, S. J. Textiles. 10th ed. New Jersey: Pearson Education, Inc., 2007.

[30] Magdassi, S.; Bassa, A.; Vinetsky, Y.; and Kamyshny, A. Silver nanoparticles as pigments for water-based ink-jet inks. Chem. Mater. 15 (2003) 2208-2217.

[31] Kim, K.; Lee, H. S.; and Kim, N. H. Silver-particle-based surface-enhanced resonance Raman scattering spectroscopy for biomolecular sensing and recognition. Anal. Bioanal. Chem. 388 (2007): 81-88.

[32] Lee, H. J.; Yeo, S. Y.; and Jeong, S. H. Antibacterial effect of nanosized silver colloidal solution on textile fabrics. J. Mater. Sci. 38 (2003): 2199-2204.

[33] Morones, J. R. et al. The bactericidal effect of silver nanoparticles. Nanotechnology 16 (2005): 2346-2353.

[34] Percival, S. L.; Bowler, P.G.; and Russell, D. Bacterial resistance to silver in wound care. J. Hosp. Infect. 60 (2005): 1-7.

[35] Senjen, R. Friends of the earth Australia.[online] (n.d.). Avaiable from: www.nano.foe.org.au.

[36] White, J. M. L.; Powell, A. M.; Brady, K.; and Russell-Jones, R. Severe generalized argyria secondary to ingestion of colloidal silver protein. Clin. .Exp. Dermatol. 28 (2003): 254-256.

[37] Braydish-Stolle, L.; Hussian, S.; Schlager, J. J.; and Hofmann, M. C. In vitro cytotoxicity of nanoparticles in mammalian germline stem cells. Toxicol. Sci. 88(2) (2005): 412-419.

[38] Hussain, S. M.; Hess, K. L.; Gearhart, J. M.; Geiss, K.T.; and Schlager, J. J. In vitro toxicity of nanoparticles in BRL 3A rat liver cells. Toxicol. In vitro. 19 (2005): 975-983.

[39] Chen, X.; and Schluesenner, H. J. Nanosilver: A nanoproduct in medical application. Toxicol. Lett. 176 (208): 1-12.

[40] Alt, V. et al. An in vitro assessment of the antibacterial properties and cytotoxicity of nanoparticulate silver bone cement. Biomaterials 25 (2004): 4383-4391.

[41] Joeng, S. H.; Hwang, Y. H.; and Yi, S. C. Antibacterial properties of padded PP/PE nonwovens incorporating nano-sized silver colloids. J. Mater. Sci. 40 (2005): 5413-5418.

[42] Pal, T.; Sau, T. K.; and Jana, N. R. Reversible formation and dissolution of silver nanoparticles in aqueous surfactant media. Langmuir 13 (1997): 1481-1485.

[43] Kapoor, S.; and Lawless, D. Reduction and aggregation of silver ions in aqueous gelatin solutions. Langmuir 10 (1994): 3018-3022.

[44] Tosun, G.; and Glicksman, H. D. Process for making finely divided particles of silver metal. US Patent 4,979,985 (1990).

[45] Fiona Turner S. et.al., Adsorption of gelatin to a polystyrene/water interface as a function of concentration, pH, and ionic strength. Langmiur, 21 (2005): 10082-10088.

[46] Zhang, Z.; Zhao, B.; and Hu, L. PVP protective mechanism of ultrafine silver powder synthesized by chemical reduction processes. J. Solid State Chem. 121 (1996): 105-110.

[47] Huang, H. H. et al. Photochemical formation of silver nanoparticles in poly(N-vinylpyrrolidone). Langmuir 12 (1996): 909-912.

[48] Vigneshwaran, N.; Nachane, R. P.; Balasubramanya, R. H.; and Varadarajan, P. V. A novel one-pot 'green' synthesis of stable silver nanoparticles using soluble starch. Carbohydr. Res. 341 (2006): 2012-2018.

[49] Voet, D.; and Voet, J. G. Biochemistry. 3rd ed. The United State of America: John Wiley & Sons Inc., 2004.

[50] Kadolph, S. J. Textiles. 10th ed. New Jersey: Pearson Education, Inc., 2007.

[51] Sang, Y. Y.; and Sung, J. H.; Preparation and characterization of polypropylene/silver nanocomposite fibers. Polym. Int. 52 (2003): 1053-1057.

CURRICULUM VITAE

Name: Miss Parichat Sudsuriya

Date of Birth: April 8, 1983   **Birth place:** Trat Province, Thailand

Address: 40/1 Moo 3, Nongchanchong, Trat-Laemsok Road, Mueang, Trat 23000, Thailand, E-mail address: chompoo_st@hotmail.com

Education:

2004   Bachelor of Science in Chemistry
King Mongkut's University of Technology Thonburi

2008   Master of Science, Program in Petrochemistry and Polymer Science, Chulalongkorn University, Thailand

Conferences:

May 2007   : 1st Polymer Graduate Conference of Thailand, Faculty of Science, Mahidol University, Thailand
"Deposition of silver nanoparticles on cotton"

October 2007   : The 33rd Congress on Science and Technology of Thailand (STT.33) Walailak University, Nakorn Si Thammarat, Thailand
"Padding of silver nanoparticles on cotton and polyester and their antibacterial efficacy"